WORKING PAPER SERIES

Temperature and Growth: a Panel Mixed Frequency VAR Analysis using NUTS2 data

Andrea Cipollini, Fabio Parla

www.recent.unimore.it

Temperature and Growth: a Panel Mixed Frequency VAR Analysis using NUTS2 data[*]

Andrea Cipollini[†]   Fabio Parla[‡]

2nd February 2023

Abstract

In this study, we contribute to the existing literature on the impact of temperature on growth by examining the orthogonalized seasonal effect jointly with the feedback from economic activity (hence treating the increase in global temperature as anthropogenic) on a sample of 225 EU NUTS2 regions. For this purpose, we use a Panel Mixed-Frequency VAR. The empirical findings show, first, a worsening impact of temperature on growth over the last sub-sample (2000-2019) relative to the full sample analysis (covering the 1981-2019 time span). Moreover, our findings show that seasonal temperature effects are not restricted only to the agriculture sector, and we also find evidence of a heterogeneous impact of seasonal temperature on growth when we turn our focus on hot and cold regions (using the average EU median annual temperature as a threshold), rich and poor regions (using the average EU median income per capita as a threshold) and between competitiveness (using the median Regional Competitiveness index as a threshold).

Keywords: Temperature shocks; seasonality; EU regional economic growth; Panel VAR

JEL: C33; Q54; R11

[†]Department of Economics, Business and Statistics, University of Palermo, V.le delle Scienze, 90128 Palermo. Email: andrea.cipollini@unipa.it. RECent and Cefin.

[‡]Department of Economics, Business and Statistics, University of Palermo, V.le delle Scienze, 90128 Palermo. Email: fabio.parla@unipa.it. (Corresponding author)

1 Introduction

The focus of this study is the analysis of the impact of rising temperature on economic growth using sub-national data for Europe. The recent report by Copernicus in the 2022 Annual Climate Summary shows, for Europe, the hottest summer ever recorded, and the highest rate of increase of any continent in the world (European temperatures have increased by more than twice the global average over the past 30 years). Therefore, it has become more stringent a prompt action by policymakers to implement the climate policies necessary to meet, in Europe, the 2030 greenhouse gas emissions net reduction intermediate target of 55% below 1990 levels, and to achieve the long-term European Green Deal target of EU-wide climate neutrality by 2050. In the baseline analysis, we use data on air temperature levels and on a proxy of real economic output observed for 225 EU NUTS2 regions over the period $1981 - 2019$. While data on regional economic activity is typically sampled at an annual frequency, temperature level series for European regions are available at a higher frequency. We construct a quarterly (i.e., seasonal) series of air temperature levels and we model the joint interactions between seasonal temperature and annual economic growth (aggregate and sector-specific) by estimating structural mixed-frequency Panel Vector Autoregressions (hereafter Panel MF-VAR).

Our contribution to the existing literature on temperature effect on growth is as follows. First, we focus on a linear seasonal effect model as an alternative to non-linear single equation model specification considered in the cross-country studies of Burke et al. (2015) and Burke et al. (2018) finding a concave relationship between temperature and income, or the one by Kahn et al. (2021) finding a different impact of positive and negative deviation from a temperature norm proxied by a moving average observed over a long-horizon.[1] To our knowledge, the only study accounting for seasonal effect is the one by Colacito et al. (2019). Our contribution to Colacito et al. (2019) is, first, based on the orthogonalization of shocks to seasonal temperature to avoid that a shock in a given season (e.g., summer) is contaminated by shocks occurring in other seasons. For this purpose, we use a structural form Mixed Frequency Panel VAR fitted to five endogenous series: four seasonal temperature series and GVA growth and identification is achieved through recursive ordering (with GVA growth ordered last).

---

[1]Studies based on sub-national data which find evidence of an inverted-U relationship between income and temperature are those by Olper et al. (2021) focusing on Italy and by Zhao et al. (2018) using 10597 global grid cells. Mohaddes et al. (2022) focus on US states using positive and negative deviation from a temperature norm in a way similar to Kahn et al. (2021).

A further contribution to Colacito et al. (2019) is the feedback from economic activity (hence treating the increase in global temperature as anthropogenic; see the study of Bansal et al., 2016, among others) given the multiple equations setting characterizing our model specification. Contrary to our study, the literature addressing the endogeneity bias of the impact of temperature on growth does not include seasonal effects, and it is based, first, on single equation panel regression, such as an autoregressive distributed lag, ARDL (see the Kahn et al., 2021 and Mohaddes et al., 2022, focusing mainly on the long-run, or the local projection studies by Acevedo et al., 2020 and by Olper et al., 2021). Second, feedback effects have been explicitly taken into account through Panel VAR. In particular, while Donadelli et al. (2021) focus on the joint interaction between temperature levels and economic growth, Alessandri and Mumtaz (2021) focus on the relationship between temperature volatility and economic growth. In particular, Alessandri and Mumtaz (2021) estimate a structural Panel VAR augmented with stochastic volatility using data for 133 countries observed over the $1960 - 2019$ time span. This methodology allows the authors to identify shocks both to the levels and the volatility of temperature and economic growth.[2] Contrary to our model specification based on mixed frequency data (in a Panel VAR context), the aforementioned studies do not include seasonal temperature effect. It is important to observe that the use of mixed frequency data allows to avoid a potential temporal aggregation bias that might arise when high-frequency data are aggregated to a lower sampling frequency (see for example Ghysels, 2016; Marcellino, 1999, for a discussion on the consequences of temporal aggregation bias in time series regressions).

An additional contribution to the literature on temperature and growth is the focus on seasonal temperature effects using sub-national data, which allow to account for the within-country heterogeneity in temperatures and growth. The need to avoid aggregation at the country level is motivated by, first, taking into account the exposure of different regions units within a country to opposing temperature shocks within a given period; second, by the wide income differences within countries. In particular, the growth-temperature relationship based on sub-national data is the focus of Deryugina and Hsiang (2014), Colacito et al. (2019), Mohaddes et al. (2022) using data for the US states. Li et al. (2019) focus on Chinese provinces; the studies of Zhao et al. (2018), Acevedo et al. (2020), Kalkuhl and Wenz (2020), Greßer et al. (2021) use sub-national data for a sample of global economies; Olper et al. (2021) focus on NUTS3 data for Italian provinces. Our focus is on 225 NUTS2 region of Europe.

Our final contribution is the analysis of heterogeneity. Several studies find evidence that a

---

[2]See also Kotz et al. (2021) study of temperature variability effect on growth using sub-national data.

temperature increase has a detrimental effect, especially in relatively hot countries, and in those relatively poor (given that they have fewer means available to adapt to further temperature increases). In particular, Dell et al. (2012) find a negative and statistically significant impact of temperature on economic growth only for poor countries. Kahn et al. (2021) find that poor countries are largely affected by temperature shocks. Nevertheless, negative effects are also found for rich countries. Furthermore, the empirical evidence in Burke and Tanutama (2019) suggests that while the negative impact of temperature exposure is much more common in poor regions, there are no meaningful variations in the response of poor and rich economies to increasing temperature. In their study on US, Colacito et al. (2019) show that the negative effect of rising temperature on GDP growth in hot states is not driven by the relatively poor states. Our final contribution is to the literature studying the heterogenous response of growth to temperature shocks by conditioning not only on hot/cold (using the average EU median annual temperature as a threshold to split the sample) and on rich/poor regions (using the average EU median income per capita as a threshold for sub-sample splitting), but also on high and low competitiveness (using the median Regional Competitiveness index as a threshold to split the sample).

Contrary to the study of Colacito et al. (2019), which finds a statistically negative effect of temperature on growth only during summer, our empirical evidence suggests a negative relationship between temperature and real GVA growth also during other seasons. Over the period $1981 - 2019$, an exogenous $1°$ Celsius increase in seasonal temperature levels leads to a contemporaneous reduction in GVA growth, particularly pronounced in summer and, to a lesser extent, in winter (although non-statistically significant). We find that the negative response of GVA growth reaches its peak typically after a one-year horizon. Moreover, the results suggest that the magnitude of the detrimental effect of increasing temperature on real economic activity is larger over a more recent sub-sample period $(2000 - 2019)$, both at aggregate and sectoral levels, showing non-negligible responses in GVA not only for agriculture, forestry and fishing sector but also for construction, industry and services. The use of panel data regressions allows us to investigate the presence of heterogeneity in the response of GVA growth to temperature shocks over different groups of regions: cold vs. hot regions, rich vs. poor regions, and highly- vs. low-competitive regions. Heterogenous temperature effects on growth show up once we account for seasonalities, that is only in the mixed-frequency Panel VAR analysis. In particular, the detrimental effects of shocks to temperature on growth during winter, summer and fall are more

4

pronounced in hot regions (e.g., those above the median temperature) than in colder ones (e.g., those below the median temperature). These findings are in line with Kahn et al. (2021) for a large number of countries and with Mohaddes et al. (2022) and Colacito et al. (2019) for US. Moreover, the negative effects of shocks to temperature on growth during each season are more pronounced in poor regions (e.g., those below the median per capita income) than in rich ones (e.g., those above the median per capita income). The only exception is summer which shows a rebound (positive and statistically significant) effect at a horizon corresponding to one year. A similar heterogeneous pattern is observed when considering low and high competitive regions (e.g., those below and above the median Regional Competitiveness index, respectively): the former are affected more negatively than the latter during winter, spring and fall. As for the summer, only on impact, there is evidence for low competitive regions of a more detrimental effect on growth than for the highly competitive ones with a rebound effect after one year. While the common frequency study of Kahn et al. (2021) finds evidence of a heterogenous temperature effect on growth only when the average world growth is introduced to control for cross-sectional dependence, our study shows the role played by seasonal effects interacting with level development (proxied by either income per capita or regional competitiveness) in driving the resilience of economic growth to temperature shocks.

Our paper is structured as follows. Section 2 describes the empirical model. Section 3 describes the empirical analysis: data and empirical findings. Section 4 discusses a number of robustness checks and Section 5 concludes.

2 Panel VAR analysis

We estimate a pooled stacked mixed-frequency Panel VAR (Panel MF-VAR) fitted to a $K_h = 1$ quarterly (seasonal) series of temperature levels and to a $K_l = 1$ macroeconomic variable observed at an annual frequency, that is every four seasons ($s = 4$):

$$Y_{i,t} = \alpha_i + \beta d_t + \sum_{\ell=1}^{p} A_{i,\ell} Y_{i,t-\ell} + u_{i,t} \tag{1}$$

where $Y_{i,t} = (T'_{i,winter}, T'_{i,spring}, T'_{i,summer}, T'_{i,fall}, \Delta y'_{i,t})'$ is a K-dimensional stacked vector of mixed-frequency variables observed for the i-th NUT2 region at year t, with $K = K_l + K_h s = 5$. The stacked vector of endogenous variables includes the quarterly series of temperature levels ($T_{i,s}$) observed for the i-th NUTS2 region during season s (i.e., winter,

spring, summer, and fall) and the annual log changes of the proxy of real economic activity ($\Delta y_{i,t}$) observed for the i-th NUTS2 region at year t. As described by Ghysels (2016), in the stacked mixed-frequency VAR the vector of endogenous variables evolves according to a standard common frequency VAR at the lowest sampling frequency available in the sample. Hence, in our case, $Y_{i,t}$ evolves according to an annual panel VAR model. Furthermore, α_i indicates the region-fixed effects, while d_t indicates the vector of annual dummies. Moreover, given that we rely on pooled estimation, the slope coefficients matrices ($A_{i,\ell}$, for $\ell = 1, \ldots, p$) associated with the lagged endogenous variables ($Y_{i,t-\ell}$) and the reduced-form residuals $u_{i,t}$ are common across regions (i.e., homogeneity assumption), that is $A_{i,\ell} = A_\ell$ and $u_{i,t} = u_t \sim \mathcal{N}(0, \Sigma)$.[3] The homogeneity assumption is imposed in our study due to the short sample length, especially when the model is estimated over the $2000 - 2019$ subsample period. We partially release this assumption by exploring the response of economic activity to temperature shocks in different groups of regions, according to the initial level of temperature, income and competitiveness degree.[4]

In the baseline specification, the proxy of real economic activity ($y_{i,t}$) is the (log of) regional real Gross Value Added (GVA).[5] Alternative proxies of regional economic activity are used: (i) (log of) real GVA by NACE sector, (ii) (log of) real GVA per capita. The model is estimated using data for an unbalanced panel of 225 NUTS2 regions in 22 EU countries, over two sample periods: (i) $1981 - 2019$ and (ii) the more recent $2000 - 2019$ sub-sample.[6] The lag length is set equal to one. We also estimate a common-frequency Panel VAR (Panel CF-VAR), where both the levels of temperature and the proxy of economic growth are observed at an annual frequency. In particular, the annual series of temperature levels is obtained by computing the mean of the four seasonal observations. For comparison, the Panel MF-VAR and the Panel CF-VAR are estimated using the same estimation samples and lag structure.

Both the MF- and Panel CF-VARs are estimated using Bayesian techniques. In particular, following Bańbura et al. (2010), we impose a Natural conjugate prior on the VAR coefficients by using artificial observations. The Gibbs sampling is used to simulate the posterior

---

[3] See Canova and Ciccarelli (2013) for a discussion on the pooled estimation with fixed effects in Panel VAR models.

[4] A similar empirical strategy is used in the study of Ciccarelli and Marotta (2021), which investigates the macroeconomic effects of climate-related transition and physical risks in 24 OECD countries over the $1990 - 2019$ time span.

[5] Data on real Gross Domestic Product (GDP) are also available in the ARDECO database. However, we prefer to use real GVA as a proxy for real economic activity whose data are also available for the different economic sectors. Results for real GDP are qualitatively and quantitatively similar to those obtained using real GVA and they are available upon request.

[6] For more details on the availability of data for each country, see Section 3.1.

distribution of the VAR parameters. The number of replications is set equal to 25000, using the last 10000 for inference (see Appendix A for technical details).[7]

The seasonal temperature shocks are identified by computing the Cholesky decomposition of the residual covariance matrix:

$$\Sigma = B_0 B_0' \qquad (2)$$

where B_0 is a lower triangular matrix containing the contemporaneous effect of the structural shocks $\varepsilon_t \sim \mathcal{N}(0, I_K)$, such that $u_t = B_0 \varepsilon_t$. In our study, the block of seasonal temperatures is ordered before the proxy of real economic activity (i.e., the growth rate of GVA). The recursive identifying scheme of the Panel VAR with the climate proxies ordered first is along the lines of the recent works of Donadelli et al. (2021), which focus on real economic activity effects of annual mean temperature, and of Alessandri and Mumtaz (2021), which focus on real economic activity effects of annual temperature volatility. Moreover, in our study, the four seasonal average temperatures are stacked into the vector of mixed-frequency variables according to the following order: $T = (T_{winter}, T_{spring}, T_{summer}, T_{fall})$. This ordering implies that an exogenous increase in the average temperature during each season affects only the following seasons.

3   Empirical analysis

3.1   Data

The mixed- and common-frequency Panel VARs are estimated using a proxy of temperature levels and of real economic growth for 225 NUTS2 regions in 22 EU countries, observed over the $1981 - 2019$ time span.[8] In the baseline specification, we use data on GVA at constant prices (deflated to 2015 price levels) as a measure of real economic activity, available at an annual frequency. The data are collected from the publicly available Annual Regional Database of the European Commission's (ARDECO database) Directorate General for Regional and Urban Policy, which is maintained and updated by the Joint Research Centre.[9] In further specifications, we use GVA at constant prices disaggregated into six

---

[7]The codes used in our paper are an adaptation of those provided by Beetsma et al. (2021) and available on Haroon Mumtaz's website .

[8]Although data on temperature levels and on economic activity are available up to 2021 for most of the regions included in the sample, we prefer to exclude the COVID-19 observations and estimate the models using data up to 2019.

[9]The database contains information on demographic and macroeconomic (including labour market, capital formation and domestic product) variables for the EU27 countries plus Albania (AL), Montenegro

NACE2 sectors: (i) agriculture, forestry and fishing, (ii) industry, excluding construction, (iii) construction, (iv) wholesale, retail, transport, accommodation and food services, information and communication, (v) financial and business services, and (vi) non-market services. As a robustness check, we estimate the model using the growth rate of the GVA per capita, computed by taking the ratio of GVA to total population (using, for the latter, data downloaded from ARDECO).

In the present study, we measure seasonal temperature effects using the level of the monthly average temperature registered during four seasons: winter (January, February, and March), spring (April, May, and June), summer (July, August, and September), and fall (October, November, and December).[10] In particular, we use monthly NUTS2-level data downloaded from the publicly-available Copernicus climate change service (C3S) operational energy dataset. The database contains climate-relevant indicators for the energy sectors, such as air temperature, among others, for 38 European countries from 1979 onward.[11] The historical dataset produces reference climate variables based on the European Centre for Medium-Range Weather Forecasts (ECMWF) Reanalysis fifth generation (ERA5) and retrieved from the Climate Data Store. Data are available both at the grid (approximately 30×30 km) and at the country (NUTS0) and regional (NUTS2) levels. Moreover, the series are available at different frequencies, that is 1 hour, 3 hours, 6 hours, daily, monthly, and yearly.[12] In our empirical application, we use the 2 meters air temperature series, which is defined as the ambient air temperature near to the surface (i.e., typically at a height of 2m). We collect the monthly (averaged) series for NUTS2 regions. The regional series are obtained by aggregating the station-level observations using both fractional land-sea mask and latitude cosine weights. The former allow accounting for the difference between land and sea grid points, while the latter account for the earth's spherical curvature. The

---

(ME), North Macedonia (MK), Norway (NO), Serbia (RS), and Turkey (TR). Data are available for all the levels of the Nomenclature of territorial units for statistics (NUTS), that is NUTS0 (corresponding to the country level), NUTS1, NUTS2 and NUTS3 (i.e., the lowest level of the territorial classification). The time series cover the period $1980 - 2023$, where the last four annual observations are forecasted based on the $2017 - 2019$ trend. Data and technical details can be found at the ARDECO online page.

[10]See Colacito et al. (2019) for a similar construction of seasonal temperature proxies.

[11]Data are available for Albania (AL), Austria (AT), Bosnia and Herzegovina (BA), Belgium (BE), Bulgaria (BG), Switzerland (CH), Cyprus (CY), Czech Republic (CZ), Germany (DE), Denmark (DK), Estonia (EE), Greece (EL), Spain (ES), Finland (FI), France (FR), Croatia (HR), Hungary (HU), Ireland (IE), Island (IS), Italy (IT), Lichtenstein (LI), Lithuania (LT), Luxembourg (LU), Latvia (LV), Montenegro (ME), North Macedonia (MK), Malta (MT), Netherlands (NL), Norway (NO), Poland (PL), Portugal (PT), Romania (RO), Serbia (RS), Sweden (SE), Slovenia (SI), Slovakia (SK), Turkey (TR), and United Kingdom (UK).

[12]The "Climate and energy indicators for Europe from 1979 to present derived from reanalysis" database is updated at a monthly frequency and it is available at https://cds.climate.copernicus.eu/cdsapp!/dataset/sis-energy-derived-reanalysis?tab=overview.

series of temperatures are measured in degrees Kelvin (K). We convert the series into degrees Celsius (°C). To estimate the common-frequency Panel VAR, the annual average temperature series is obtained by averaging out the four seasonal observations in each year. The final dataset includes regional observations of temperature levels and of real GVA growth rate for 22 EU countries and it is constructed as follows.[13] First, we exclude from the initial sample of 33 countries (that is the maximum geographical coverage for which information on both economic activity and temperature is available) the ones that consist of only one NUTS2 region (i.e., no distinction between NUTS levels): Cyprus, Estonia, Luxembourg, Latvia, Montenegro, North Macedonia, and Malta. Moreover, we exclude Albania, Norway, Serbia, and Turkey since they are not EU members. Finally, since data on 2m air temperature are not available for *Région de Bruxelles-Capitale* (BE10), *Bremen* (DE50), *Ciudad Autónoma de Ceuta* (ES63), *Ciudad Autónoma de Melilla* (ES64), *Guadeloupe* (FRY1), *Martinique* (FRY2), *Guyane* (FRY3), *La Réunion* (FRY4), *Mayotte* (FRY5), and Região Autónoma dos Açores (PT20), we remove these regions from the estimation sample.

To investigate whether the temperature levels increased in the 225 NUTS2 regions over the $1981 - 2019$ period, we follow Kahn et al. (2021) and Mohaddes et al. (2022) and we regress the temperature levels on a constant term and a deterministic linear time trend for each NUTS2 region.[14] The region-specific coefficients associated with the time trend, which measure to what extent the temperature has increased on average per year, are reported in Figure 1. We report the results for the seasonal temperatures as well as for the annual (averaged) temperature. As can be seen in Figure 1, temperature levels observed in each season increased over the $1981 - 2019$ time span, in almost all the NUTS2 regions. The largest average (across NUTS2 regions) per annum increase in temperature levels has been observed in spring (0.0522), followed by winter (0.0393), fall (0.0391), and summer (0.0368), while the average (across NUTS2) rise in annual temperature is equal to 0.0419

---

[13]The 22 EU countries are: Austria (AT), Belgium (BE), Bulgaria (BG), Czech Republic (CZ), Germany (DE), Denmark (DK), Greece (EL), Spain (ES), Finland (FI), France (FR), Croatia (HR), Hungary (HU), Ireland (IE), Italy (IT), Lithuania (LT), Netherlands (NL), Poland (PL), Portugal (PT), Romania (RO), Sweden (SE), Slovenia (SI), and Slovakia (SK). In the baseline specification, we deal with an unbalanced panel of observations given that data availability differs both between and within countries, especially for macroeconomic data. The largest sample is observed in 11 countries (i.e., $1981 - 2019$), including AT, BE, DE, DK, ES, FI, FR, IT, NL, PT, SE, while the smallest one is reported by EL and HR (i.e., $1996 - 2016$). Moreover, in Germany, 8 regions out of the 38 NUTS2 territories report data only from 1992 onward.

[14]As in Kahn et al. (2021) and Mohaddes et al. (2022), the region-specific regression has the following representation: $T_{i,t} = \alpha_i + \beta_i t + u_{i,t}$, where $T_{i,t}$ is the temperature levels observed in region i at year t, during each of four seasons individually (winter, spring, summer, and fall) as well as over the year (annual average), for $i = 1, \ldots, 225$. Moreover, β_i is the region-specific coefficient associated with the linear time trend and it measures the per annum average rise in temperature levels reported by the i-th region.

Figure 1: Estimates of the average increase in temperature levels over the $1981 - 2019$ time period.
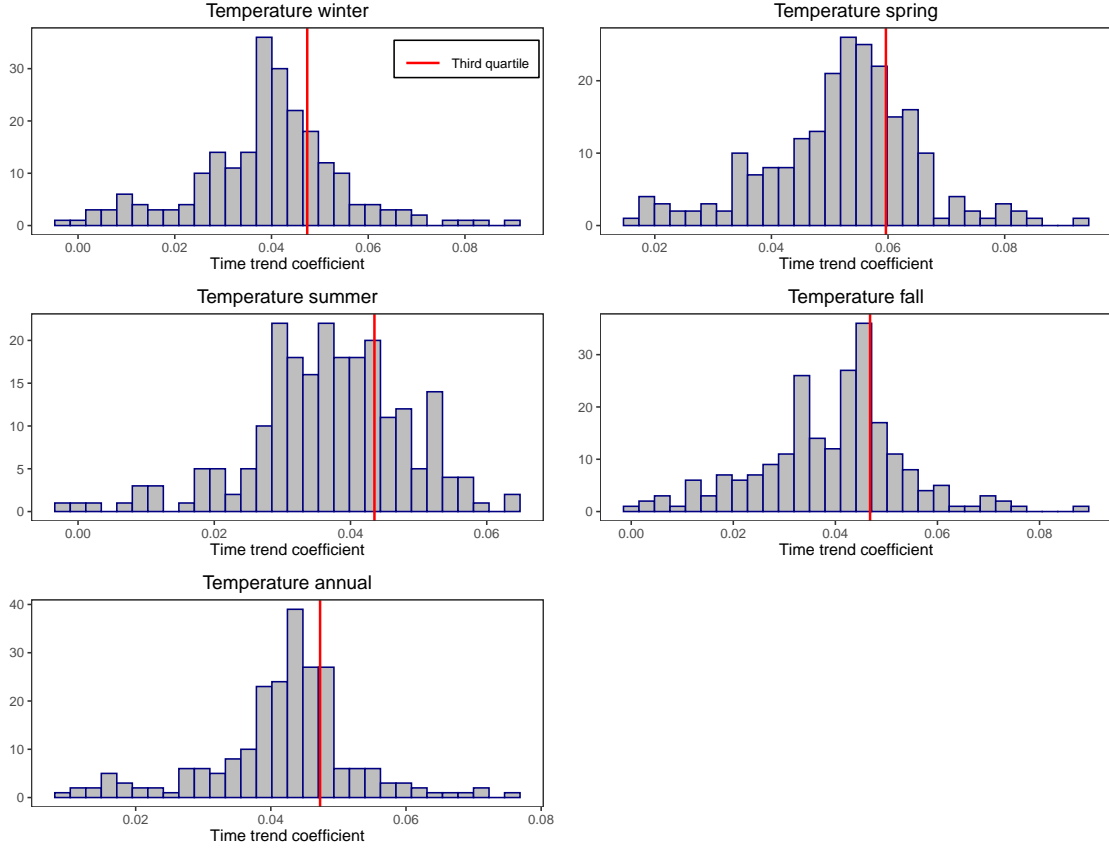
Notes. Distribution of the estimate of the coefficients associated with the deterministic time trend (β_i) of the following regression: $T_{i,t} = \alpha_i + \beta_i t + u_{i,t}$, where $T_{i,t}$ is the temperature levels observed in each of four seasons individually (winter, spring, summer, and fall) and the averaged yearly temperature (annual). The third quartile for winter (0.0474), spring (0.0596), summer (0.0435), fall (0.0468), as well as for the average annual series (0.0473) is also reported (red line).

per annum.

3.2   Aggregate GVA results

In line with Greßer et al. (2021) study based on sub-national data, results in Table 1 do not show evidence that temperature and regional economic development across the 225 NUTS2 European regions follow an inverted U-shape. As an alternative to the non-linear single equation model specification, we use a multiple linear equation setting with seasonal effects captured through the Panel Mixed-Frequency VAR.

Table 1: Non-linear effect of temperature level on real economic growth, over the $1981 - 2019$ period.
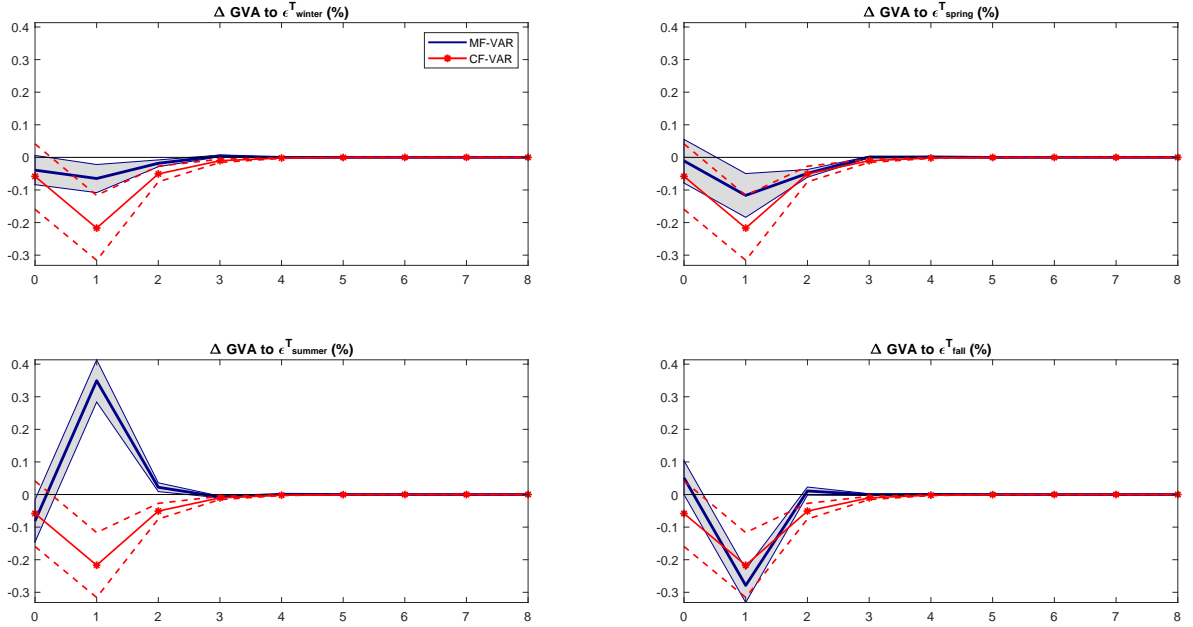
	Annual	Winter	Spring	Summer	Fall
T	0.1453	0.0654**	0.4224*	0.5648	0.2553***
	(0.2562)	(0.0268)	(0.2347)	(0.4182)	(0.0610)
T^2	0.0210	0.0305***	−0.0106	−0.0198	0.0027
	(0.0137)	(0.0034)	(0.0083)	(0.0121)	(0.0046)

Notes. Estimated coefficients (in percent) associated with the level of annual temperature (and its squared term) (column 1) and with the level of seasonal temperatures (and their squared term) (columns $2-5$) obtained from the estimation of the following regressions: (i) $\Delta y_{i,t} = \alpha_i + \beta_i t + \theta T_{i,t} + \phi T_{i,t}^2 + u_{i,t}$, where $T_{i,t}$ is the averaged yearly temperature (annual); (ii) $\Delta y_{i,t} = \alpha_i + \beta_i t + \sum_{s=1}^{4} \theta_s T_{i,s,t} + \sum_{s=1}^{4} \phi_s T_{i,s,t}^2 + u_{i,t}$, where $T_{i,s,t}$ is the level of temperature observed in each season s (winter, spring, summer, and fall). Moreover, $\Delta y_{i,t}$ is the growth rate of real GVA and β_i is the coefficient of the region-specific linear time trend. The estimation sample is $1981 - 2019$. Standard errors clustered by region are in parentheses. Significance at the 1% (***), 5% (**), and 10% (*) levels are also reported.

In this section, we discuss the empirical findings for the baseline specification (based on the full sample observed over the period $1981 - 2019$ for a panel of 225 NUTS2 regions). In particular, we report the impulse response functions of the real GVA growth rate (ΔGVA) to temperature shocks (ε^T) proxied by an exogenous increase in the 2m air temperature. The impulse responses are normalised to an increase of 1°C (on impact) both in the Panel MF-VAR (i.e., a unitary increase in the temperature level in each of the four seasons) and in the Panel CF-VAR, and they are computed over an 8-year forecast horizon.[15] Figure 2 shows the structural impulse responses of ΔGVA to a 1°C increase in the level of temperature observed during each of the four seasons (i.e., winter, spring, summer, and fall). In each chart, we report the median response (blue line) and the corresponding 68% error bands (grey shadow area) obtained from the estimation of the Panel MF-VAR fitted

---

[15]As a robustness check, we follow Colacito et al. (2019) and we estimate the Panel MF-VAR fitted to ΔGVA and deseasonalized temperature series. The latter is computed as follows. First, we estimate the following panel regression: $T_{i,d} = \sum_{m=1}^{12} \gamma_m I_{i,m} + \alpha_i + u_{i,d}$, where $T_{i,d}$ is the temperature levels in region i and day d, $I_{i,m}$ is a dummy for month m in region i, α_i are region-fixed effects, and $u_{i,d}$ is the error term. Then, we compute the residuals from the estimated panel regression and aggregate them at a monthly frequency. Finally, the four seasonal deseasonalized temperature series are obtained by averaging out the three monthly observations. The results of the Panel MF-VAR (and of the Panel CF-VAR) fitted to ΔGVA and to the deseasonalized temperature levels are qualitatively and quantitatively similar to those obtained by using the raw temperature levels and they are available upon request.

Figure 2: Responses of the regional real GVA growth.

Notes. Impulse responses of the real GVA growth rate (ΔGVA) in percent, computed over an 8-year forecast horizon, using the $1981 - 2019$ period as estimation sample. The charts show the impulse response profile of ΔGVA to temperature shocks occurring in winter (ε_{winter}^T), spring (ε_{spring}^T), summer (ε_{summer}^T), and fall (ε_{fall}^T). Each chart displays the median response (blue line) and the corresponding 68% error bands (grey shadow area) computed by estimating the Panel MF-VAR described in equation (1). The size of the temperature shocks in each season is normalized to a 1°C increase in the temperature levels. The median response (red line with asterisk) obtained from the estimation of a Panel CF-VAR (fitted to annual temperature and real GVA growth rate) and the corresponding 68% error bands (red dashed lines) are also reported. For comparison, the size of the shock in the Panel CF-VAR is also normalized to a 1°C increase in the level of temperature.

to the four seasonal time series of temperature level and to the annual log changes of real GVA. For comparison, in Figure 2 we also report the impulse response obtained from the estimation of a Panel CF-VAR (median response and 68% error bands in red lines) fitted to annual series of temperature levels and ΔGVA, where the former is obtained by averaging out the four seasonal observations. The inefficiency factor computed over the 10000 retained draws is relatively low, suggesting evidence of convergence of the Gibbs sampling algorithm (see Appendix B).
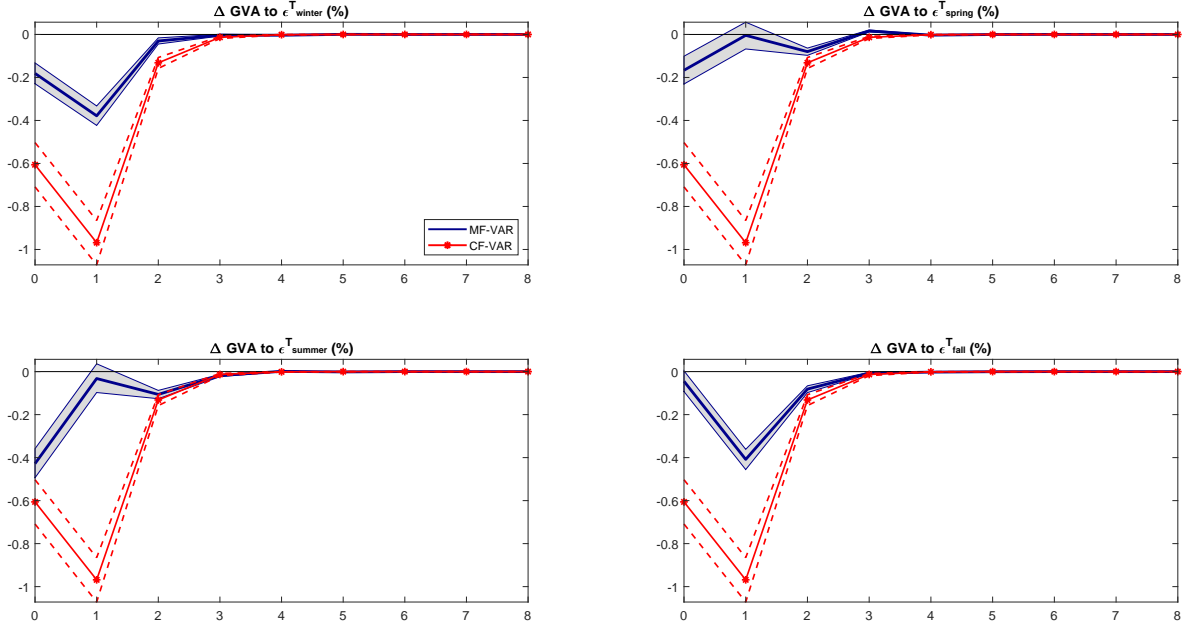
We can observe, from Figure 2, that the response of the annual ΔGVA to an increase in the annual temperature levels (i.e., the response obtained from the Panel CF-VAR)

is negative over the whole forecast horizon. On impact, we find a reduction of 0.06% (although it is not statistically significant), while the negative response of ΔGVA reaches its peak after a 2-year horizon (-0.22%), before dying out after 4 years. A closer inspection of the seasonal responses of ΔGVA to temperature shocks (i.e., the response obtained from the Panel MF-VAR) reveals that summer (-0.08%) and, to a lesser extent, winter (-0.04%, although with uncertainty around the median estimates) contribute the most to the aforementioned reduction observed on impact in the annual ΔGVA, while the response in spring and in fall is not statistically different from zero. The negative contemporaneous impact of rising temperature in summer on economic output is in line with the empirical evidence provided by Colacito et al. (2019) for US.[16] Beyond time zero, we observe a reduction of the economic growth in all the seasons with the only exception of the summer where we observe a rebound effect at horizon one (0.35%). At horizon one, the largest reduction of ΔGVA is observed in fall (-0.28%), with a magnitude in the response that is similar to that obtained from the estimation of the Panel CF-VAR, followed by the response in spring (-0.12%) and in winter (-0.06%). Finally, the response of ΔGVA diminishes after a 2-year forecast horizon in all four seasons.

To assess whether the joint relationship between temperature levels and real economic growth has changed over the estimation sample, we repeat the empirical analysis using a more recent sub-sample of 20 years, that is $2000-2019$. Figure 3 shows the responses of ΔGVA to temperature shocks obtained from the estimation of both the Panel MF-VAR and the Panel CF-VAR. As can be seen from Figure 3, overall, the negative effect of a $1°C$ rise in the levels of temperature on economic growth is larger (in absolute values) than that observed over the full sample, i.e. $1981-2019$ (see Figure 2), using both annual (Panel CF-VAR) and seasonal (Panel MF-VAR) series of temperature. In the case of Panel CF-VAR, we find that ΔGVA decreases by 0.61%, on impact, which is ten times the response observed using the $1981-2019$ sample period. Likewise the results observed using data for $1981-2019$, the peak of the negative response is reached after one year also over the sub-sample period: -0.97% (i.e., more than four times the response estimated over the full sample). Then, the response of the ΔGVA approaches zero over the next two forecast horizons.

---

[16]In their study, Colacito et al. (2019) also estimate the impact of an increase in the annual (averaged) temperature on economic activity, finding a not statistically significant effect of temperature on GDP for the U.S. states. However, once the authors replace the annual series of temperatures with the seasonal ones, the relationship turns out to be statistically significant pointing to the importance of using higher frequency data in studying the macroeconomic effects of temperature shocks.

Figure 3: Sub-sample analysis: responses of the regional real GVA growth over the $2000-2019$ period.

Notes. Impulse responses of the real GVA growth rate (ΔGVA) in percent, computed over an 8-year forecast horizon, using the $2000-2019$ period as estimation sample. The charts show the impulse response profile of ΔGVA to temperature shocks occurring in winter (ε_{winter}^{T}), spring (ε_{spring}^{T}), summer (ε_{summer}^{T}), and fall (ε_{fall}^{T}). Each chart displays the median response (blue line) and the corresponding 68% error bands (grey shadow area) computed by estimating the Panel MF-VAR described in equation (1). The size of the temperature shocks in each season is normalized to a 1°C increase in the temperature levels. The median response (red line with asterisk) obtained from the estimation of a Panel CF-VAR (fitted to annual temperature and real GVA growth rate) and the corresponding 68% error bands (red dashed lines) are also reported. For comparison, the size of the shock in the Panel CF-VAR is also normalized to a 1°C increase in the level of temperature.

The results obtained from the mixed-frequency analysis reveal interesting findings. On impact, the responses of economic growth to temperature shocks are negative and statistically significant in all seasons. Moreover, they show a large negative magnitude than those obtained over the $1981-2019$ estimation sample. As in the full sample analysis, the empirical evidence suggests the largest contribution of the summer in the reduction of annual ΔGVA (i.e., the one observed using the annual temperature series). In particular, the response of ΔGVA to a 1°C rise in the temperature levels observed in summer is largest at horizon zero (-0.43%), before diminishing over the following three years. A

relatively large (negative) response is observed also in winter (-0.18%) and, to a lesser extent, in spring (-0.17%), while it is smaller in fall (-0.04%). The peak of the negative response of ΔGVA at horizon one obtained from the Panel CF-VAR is explained by the reduction of economic growth observed in winter (-0.38%) and in fall (-0.41%). Similar to the impulse response profile of ΔGVA to annual temperature shocks, also the seasonal responses converge to zero after three/four years.

3.3   Economic sectoral results

Figures 4-9 show the responses of ΔGVA reported for different economic sectors. On impact, the economic sectors that contribute the most to the reduction observed in the aggregate ΔGVA are agriculture, forestry and fishing (-1.95%), industry (-1.72%) and, to a lesser extent, non-market services (-0.45%). These results are in line with Acevedo et al. (2020) which find that the negative effect of rising temperature on GVA growth is not limited to agriculture, but it is also extended to manufacturing.[17] The response of the proxy of economic activity is not statistically different from zero in construction, wholesale/retail, transport and other services, while the financial & business sector seems to be positively affected by an increase in the levels of temperature, at least on impact. The positive response observed in the financial & business sector on impact is in line with the findings discussed in Mohaddes et al. (2022), which find that positive deviations of temperature from the moving average long-term historical mean (i.e., climate norm) positively affect US GDP in the financial sector.[18] Moreover, a mild detrimental effect of temperature shocks on the services sector's value added is also documented in Acevedo et al. (2020). At horizon one (i.e., the negative peak in the response of ΔGVA to annual temperature shocks), we find a reduction of ΔGVA in most of the economic sectors: construction (-4.38%), wholesale/retail, transport and other services (-2.08%), industry (-1.53%), financial & business services (-0.64%), and non-market services (-0.08%, although it is not statistically significant). The only exception is agriculture (4.07%), where we observe a rebound effect. The positive response of ΔGVA in agriculture is in line with Alessandri and Mumtaz (2021) that finds positive although short-lived effects of temperature volatility

---

[17]However, it is important to note that, differently from Acevedo et al. (2020), in our empirical analysis the industry sector includes: (*i*) mining and quarrying, (*ii*) manufacturing, (*iii*) electricity, gas, steam and air conditioning supply, (*iv*) water supply, sewerage, waste management and remediation activities.

[18]The authors argue that these results might be due to an increase in the insurance premiums for climate change.

shocks on agricultural GVA.[19]

We now turn our focus to the results obtained from the Panel MF-VAR. On impact, we find that the largest reduction in economic growth is observed in summer for most of the economic sectors, including agriculture (-2.37%), construction (-1.59%), industry (-0.78%), and non-market services (-0.32%). The response of ΔGVA observed in summer is not statistically significant for wholesale/retail, transport and other services and for financial & business services. Moreover, for agriculture, industry and non-market services, we find a reduction in economic activity also in most of the remaining seasons. In particular, we observe a detrimental effect in ΔGVA for agriculture (-0.44% in spring and -0.41% in fall), for industry (-0.46% in winter, -0.49% in spring, and -0.31% in fall), and for non-market services (-0.16% in winter and -0.11% in spring). For other economic sectors, such as construction, wholesale/retail, transport and other services, and financial & business services, we observe a positive and statistically significant response of economic growth to temperature shocks. However, most of these responses become negative at horizon one, with a cumulative response over the two-year horizon that remains negative. For example, in the construction sector, the positive response observed in winter (0.47%) and in spring (0.41%) is more than offset by the reduction reported after a one-year horizon, that is -1.69% and -0.89%, respectively. Likewise, for wholesale/retail, transport and other services, the increase in ΔGVA observed, on impact, in spring (0.23%) is followed by a reduction of 0.57%, at horizon one. Moreover, for financial & business services, we observe a negative cumulative effect of temperature rise on economic activity over a two-year horizon only in summer: the increase of ΔGVA observed on impact (0.09%) is followed by a reduction of 0.34% at horizon one. In the remaining seasons, the negative response of GVA at horizon one is not offset by the increase observed on impact: winter (0.26% on impact and -0.13% at horizon one), in spring (0.13% on impact and -0.09% at horizon one), and in fall (0.65% on impact and -0.21% at horizon one).

Beyond time zero, with the only exception of agriculture, where we observe a large rebound effect (similar to that observed from the estimation of the Panel CF-VAR), the results show a negative impact of temperature shocks on ΔGVA. The most affected sectors are construction (-1.69% in winter, -0.89% in spring, -0.47% in summer, and -0.98% in fall), wholesale/retail, transport and other services (-0.55% in winter, -0.57% in spring, -0.21% in summer, and -0.66% in fall), and industry (-0.60% in winter and -0.64% in fall). Negative responses are also observed for financial & business services (-0.13% in

---

[19]As stated by Alessandri and Mumtaz (2021), this result could be explained by a relatively large increase in the price of final goods.

Figure 4: Sub-sample analysis: responses of the regional real GVA growth in agriculture over the $2000 - 2019$ period.
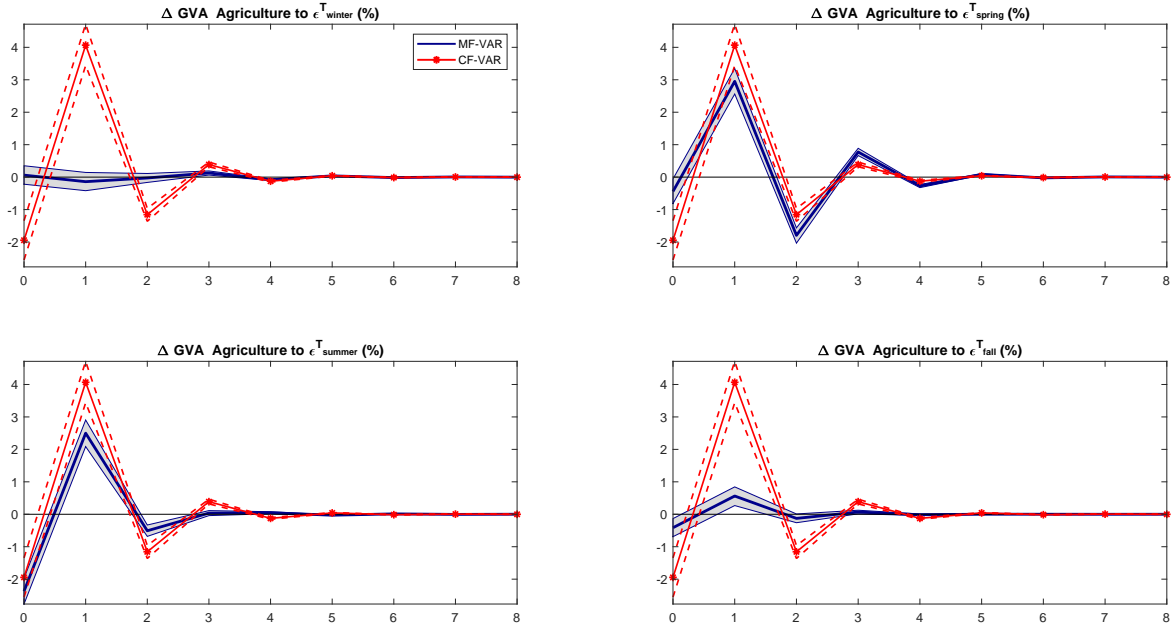
Notes. Impulse responses of the real GVA growth rate in agriculture, forestry and fishing (ΔGVA Agriculture) in percent, computed over a 8-year forecast horizon, using the $2000 - 2019$ period as estimation sample. The charts show the impulse response profile of ΔGVA Agriculture to temperature shocks occurring in winter (ε_{winter}^T), spring (ε_{spring}^T), summer (ε_{summer}^T), and fall (ε_{fall}^T). Each chart displays the median response (blue line) and the corresponding 68% error bands (grey shadow area) computed by estimating the Panel MF-VAR described in equation (1). The size of the temperature shocks in each season is normalized to a $1°C$ increase in the temperature levels. The median response (red line with asterisk) obtained from the estimation of a Panel CF-VAR (fitted to annual temperature and ΔGVA Agriculture) and the corresponding 68% error bands (red dashed lines) are also reported. For comparison, the size of the shock in the Panel CF-VAR is also normalized to a $1°C$ increase in the level of temperature.

winter, -0.09% in spring, -0.34% in summer, and -0.21% in fall) and, to a lesser extent, for non-market services (-0.14% in fall).

Figure 5: Sub-sample analysis: responses of the regional real GVA growth in industry over the $2000 - 2019$ period.
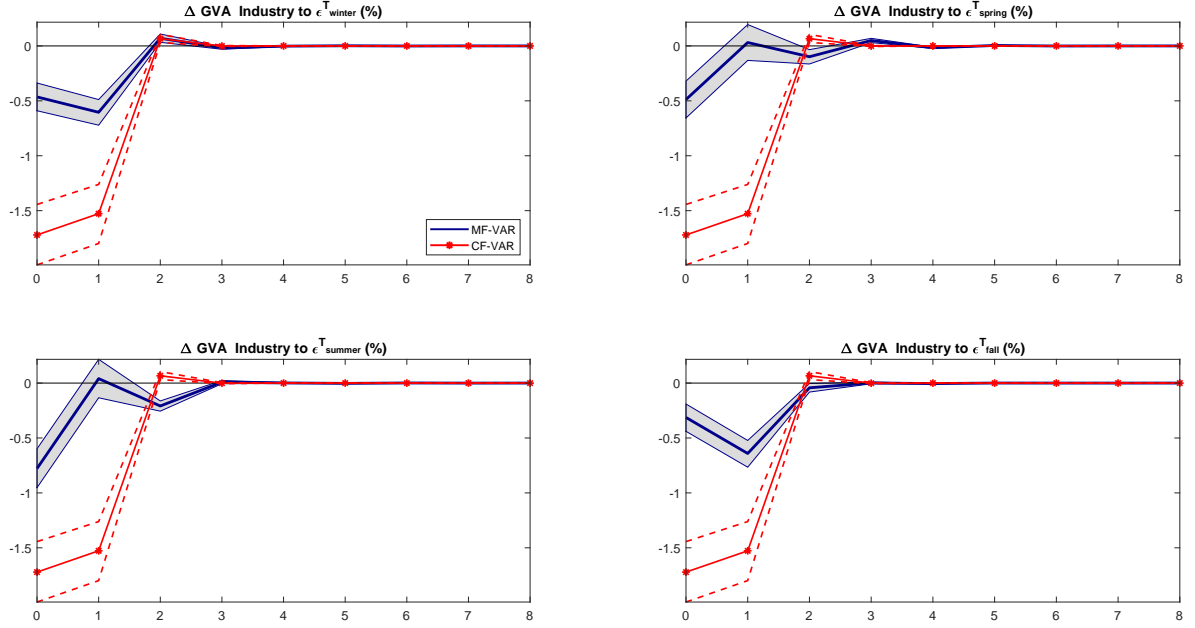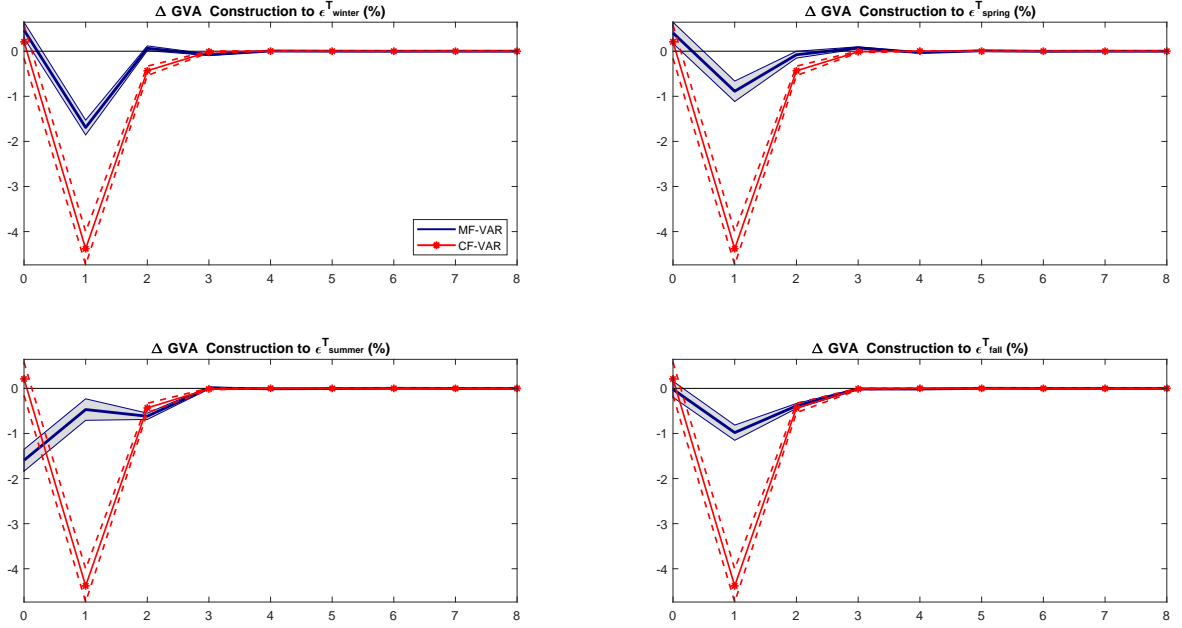

Notes. Impulse responses of the real GVA growth rate in industry, excluding construction (ΔGVA Industry) in percent, computed over a 8-year forecast horizon, using the $2000 - 2019$ period as estimation sample. The charts show the impulse response profile of ΔGVA Industry to temperature shocks occurring in winter (ε^T_{winter}), spring (ε^T_{spring}), summer (ε^T_{summer}), and fall (ε^T_{fall}). Each chart displays the median response (blue line) and the corresponding 68% error bands (grey shadow area) computed by estimating the Panel MF-VAR described in equation (1). The size of the temperature shocks in each season is normalized to a $1°$C increase in the temperature levels. The median response (red line with asterisk) obtained from the estimation of a Panel CF-VAR (fitted to annual temperature and ΔGVA Industry) and the corresponding 68% error bands (red dashed lines) are also reported. For comparison, the size of the shock in the Panel CF-VAR is also normalized to a $1°$C increase in the level of temperature.

3.4 Heterogeneity

In this section, we investigate the presence of heterogeneity in the response of real economic activity to a $1°$C increase in the temperature levels across the 225 NUTS2 regions. In particular, we study whether the regional average responses of ΔGVA are driven by (i) the temperature levels, (ii) the income levels, or (iii) the degree of competitiveness of the NUTS2 regions. In particular, we follow Kahn et al. (2021) and we conduct two empirical exercises: in a first empirical exercise, the 225 NUTS2 regions are grouped into "hot" and "cold" regions, according to their average ($2000 - 2019$) temperature levels, while in a

Figure 6: Sub-sample analysis: responses of the regional real GVA growth in construction over the $2000 - 2019$ period.

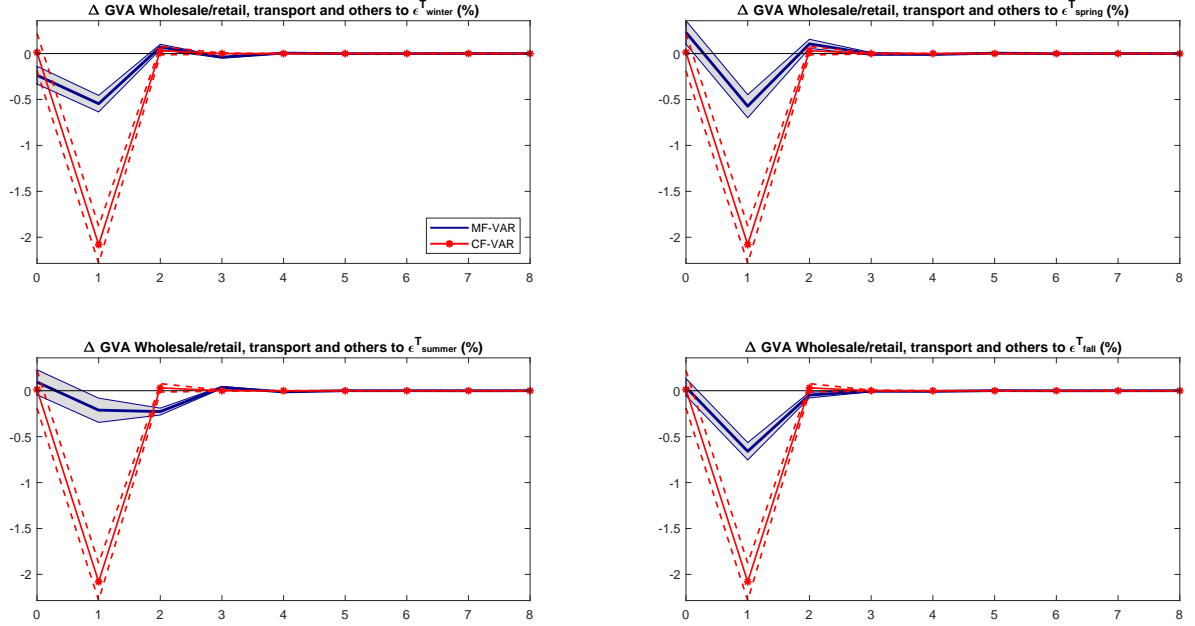**Notes**. Impulse responses of the real GVA growth rate in construction (ΔGVA Construction) in percent, computed over a 8-year forecast horizon, using the $2000 - 2019$ period as estimation sample. The charts show the impulse response profile of ΔGVA Construction to temperature shocks occurring in winter (ε_{winter}^{T}), spring (ε_{spring}^{T}), summer (ε_{summer}^{T}), and fall (ε_{fall}^{T}). Each chart displays the median response (blue line) and the corresponding 68% error bands (grey shadow area) computed by estimating the Panel MF-VAR described in equation (1). The size of the temperature shocks in each season is normalized to a $1°C$ increase in the temperature levels. The median response (red line with asterisk) obtained from the estimation of a Panel CF-VAR (fitted to annual temperature and ΔGVA Construction) and the corresponding 68% error bands (red dashed lines) are also reported. For comparison, the size of the shock in the Panel CF-VAR is also normalized to a $1°C$ increase in the level of temperature.

second empirical exercise, we split the sample of NUTS2 regions into two sub-groups based on the average ($2000 - 2019$) income levels, proxied by the GVA at purchasing power parity (PPP) per capita, i.e., "rich" and "poor" regions. Furthermore, a third empirical exercise is conducted by grouping the NUTS2 regions into two sub-groups, i.e., "highly" and "low" competitive regions, on the basis of the European regional competitiveness index (RCI) constructed by the European Commission.

To investigate whether hotter regions are affected by temperature shocks more than colder regions, we split the sample of 225 NUTS2 regions into two sub-groups: "hot" and "cold"

Figure 7: Sub-sample analysis: responses of the regional real GVA growth in wholesale, retail, transport, accommodation and food services, information and communication over the $2000 - 2019$ period.

Notes. Impulse responses of the real GVA growth rate in wholesale, retail, transport, accommodation and food services, information and communication, (ΔGVA Wholesale/retail, transport and others) in percent, computed over a 8-year forecast horizon, using the $2000 - 2019$ period as estimation sample. The charts show the impulse response profile of ΔGVA Wholesale/retail, transport and others to temperature shocks occurring in winter (ε_{winter}^{T}), spring (ε_{spring}^{T}), summer (ε_{summer}^{T}), and fall (ε_{fall}^{T}). Each chart displays the median response (blue line) and the corresponding 68% error bands (grey shadow area) computed by estimating the Panel MF-VAR described in equation (1). The size of the temperature shocks in each season is normalized to a 1°C increase in the temperature levels. The median response (red line with asterisk) obtained from the estimation of a Panel CF-VAR (fitted to annual temperature and ΔGVA Wholesale/retail, transport and others) and the corresponding 68% error bands (red dashed lines) are also reported. For comparison, the size of the shock in the Panel CF-VAR is also normalized to a 1°C increase in the level of temperature.

regions. The two sub-groups are constructed as follows. For each NUTS2 region, first, we compute the annual temperature levels by averaging out the four seasonal temperature series. Then, for each region, we compute the mean of the annual temperature levels over the period $2000 - 2019$. A region is defined as a "hot" region if its average annual temperature level is above the median, while a region is labelled as a "cold" region if its

Figure 8: Sub-sample analysis: responses of the regional real GVA growth in Financial & business services over the $2000 - 2019$ period.
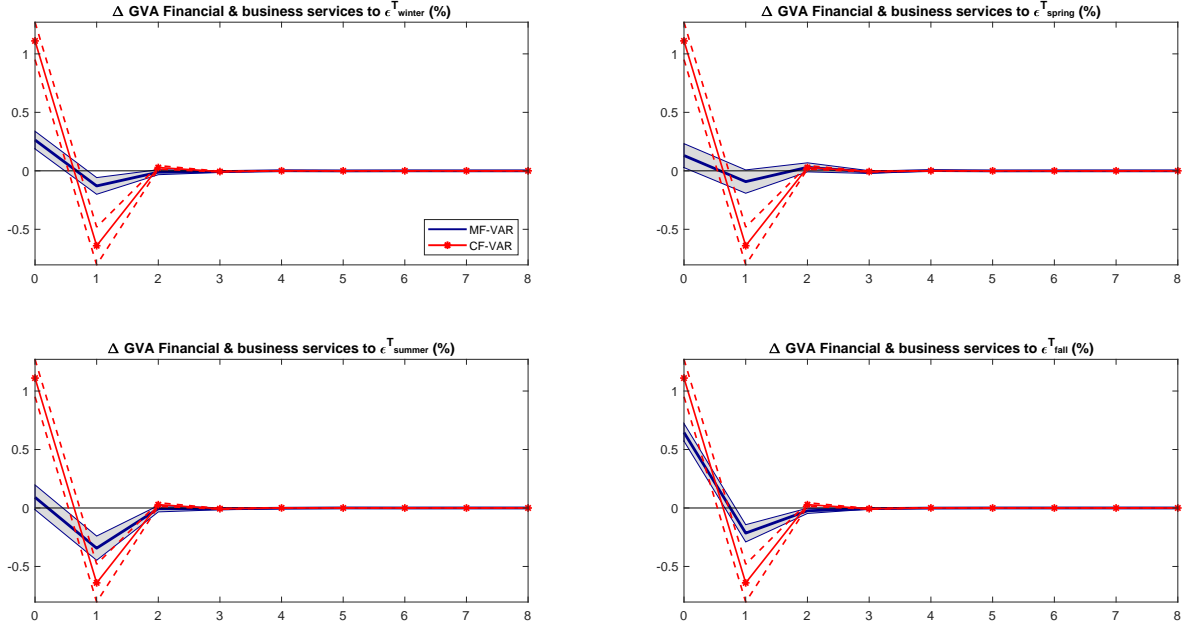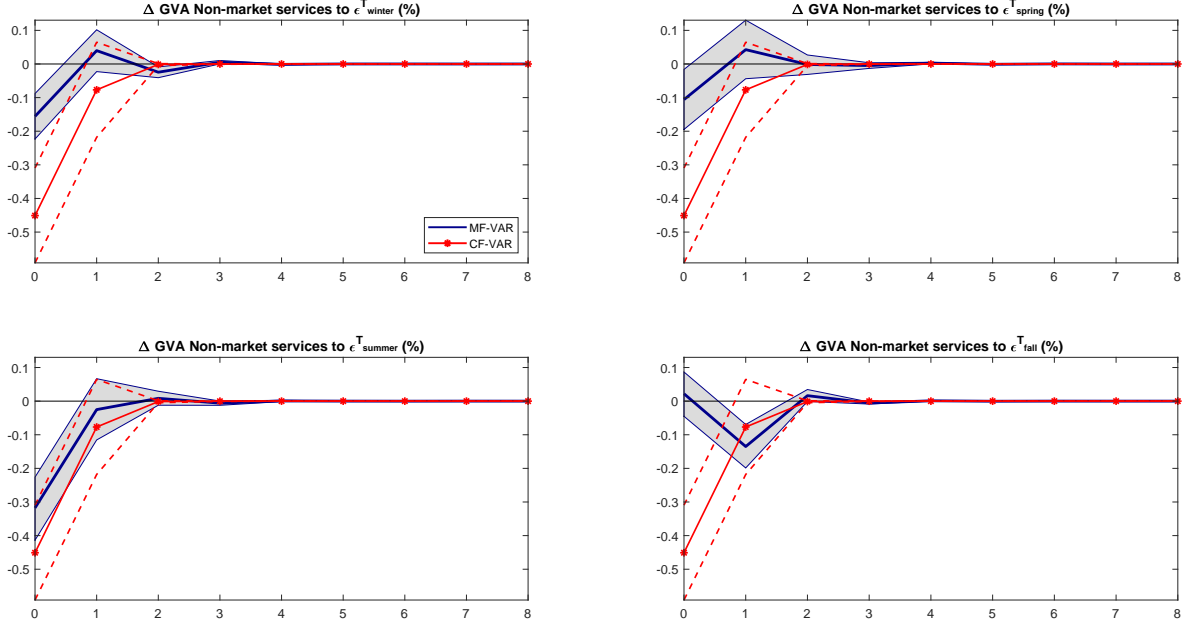

Notes. Impulse responses of the real GVA growth rate in Financial & business services, (ΔGVA Financial & business services) in percent, computed over a 8-year forecast horizon, using the $2000 - 2019$ period as estimation sample. The charts show the impulse response profile of ΔGVA Financial & business services to temperature shocks occurring in winter (ε_{winter}^T), spring (ε_{spring}^T), summer (ε_{summer}^T), and fall (ε_{fall}^T). Each chart displays the median response (blue line) and the corresponding 68% error bands (grey shadow area) computed by estimating the Panel MF-VAR described in equation (1). The size of the temperature shocks in each season is normalized to a 1°C increase in the temperature levels. The median response (red line with asterisk) obtained from the estimation of a Panel CF-VAR (fitted to annual temperature and ΔGVA Financial & business services) and the corresponding 68% error bands (red dashed lines) are also reported. For comparison, the size of the shock in the Panel CF-VAR is also normalized to a 1°C increase in the level of temperature.

average annual temperature level is below the median.[20] Hot and cold regions are shown in Figure 10. Figure 11 shows the responses of aggregate ΔGVA to temperature shocks reported in cold (Figure 11, panel a) and hot (Figure 11, panel b) NUTS2 regions.

We first describe the results obtained from the Panel CF-VAR fitted to the annual series of temperature levels and ΔGVA. As shown by Figure 11, both the cold and the hot regions report a negative response in economic growth to a 1°C increase in the level of annual temperature. Over the whole forecast horizon, the negative response reported in cold

---

[20]The median of the average (2000-2019) annual temperature levels is equal to 10.51°C.

Figure 9: Sub-sample analysis: responses of the regional real GVA growth in Non-market services over the $2000 - 2019$ period.
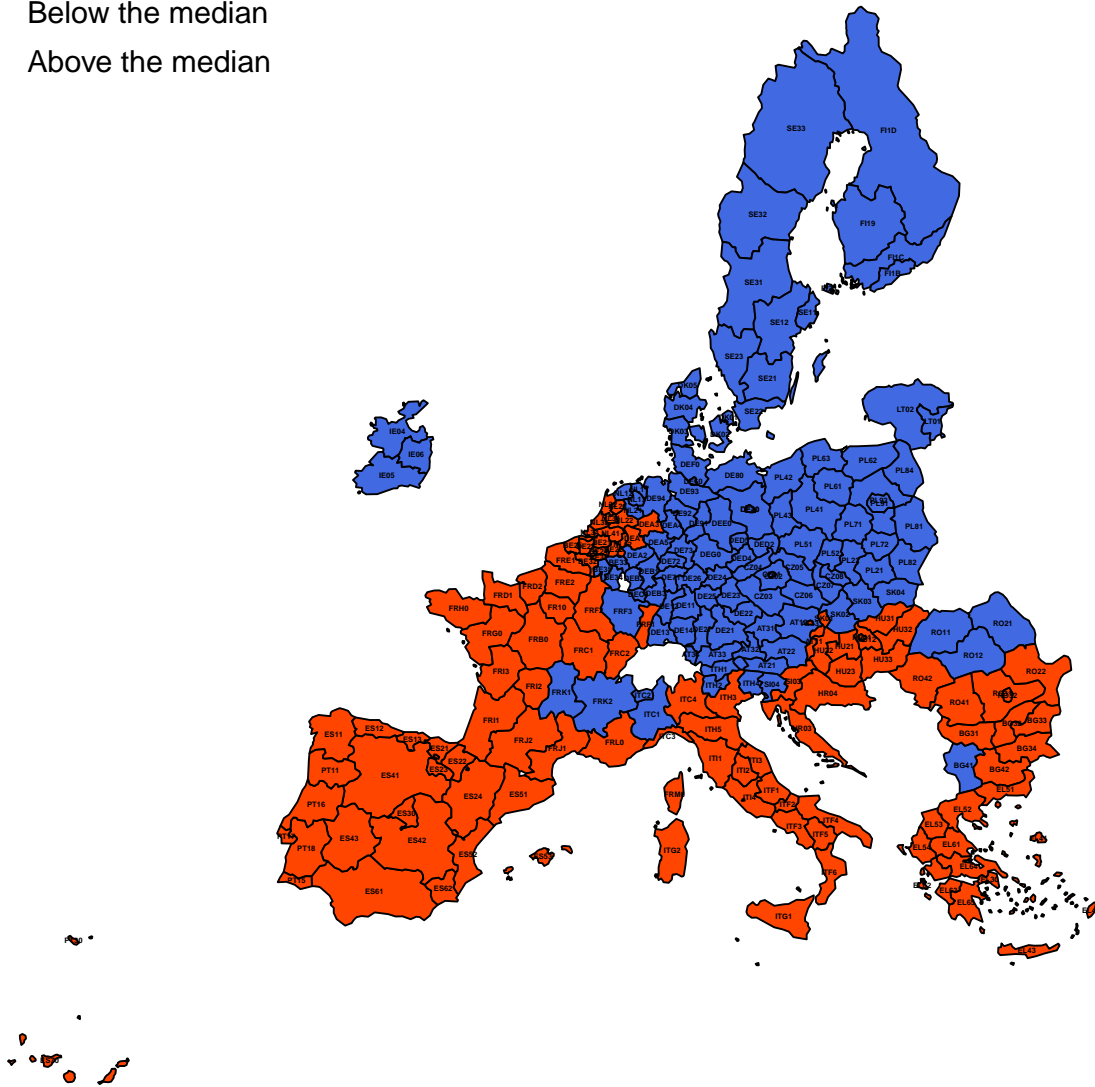

Notes. Impulse responses of the real GVA growth rate in Non-market services, (ΔGVA Non-market services) in percent, computed over a 8-year forecast horizon, using the $2000 - 2019$ period as estimation sample. The charts show the impulse response profile of ΔGVA Non-market services to temperature shocks occurring in winter (ε^T_{winter}), spring (ε^T_{spring}), summer (ε^T_{summer}), and fall (ε^T_{fall}). Each chart displays the median response (blue line) and the corresponding 68% error bands (grey shadow area) computed by estimating the Panel MF-VAR described in equation (1). The size of the temperature shocks in each season is normalized to a $1°C$ increase in the temperature levels. The median response (red line with asterisk) obtained from the estimation of a Panel CF-VAR (fitted to annual temperature and ΔGVA Non-market services) and the corresponding 68% error bands (red dashed lines) are also reported. For comparison, the size of the shock in the Panel CF-VAR is also normalized to a $1°C$ increase in the level of temperature.

regions is slightly larger, in absolute values, than that observed for hot regions (although there is an overlap in the error bands). In particular, on impact, ΔGVA decreases by 0.65% in cold regions, while the reduction observed in the hot regions is equal to -0.57%. At horizon one (that is the peak of the negative response), we find that an increase in temperature levels is associated with a reduction of 0.97% in cold regions and of 0.82% in hot regions. Notwithstanding, the results from the Panel CF-VAR suggest that colder regions are affected more negatively than hotter regions by rising the (average) annual temperature levels, the impulse response analysis conducted by estimating the Panel

Figure 10: Hot and cold NUTS2 regions. Annual temperature levels over the $2000 - 2019$ time span.

Notes. Annual temperature levels of the 225 EU NUTS2 regions averaged over the period $2000 - 2019$. A region is labelled as a cold region if its average temperature is below the median (that is $10.51°C$), otherwise, the region falls into the hot region sub-group. The Eurostat NUTS 2021 code for each region is also reported.

Figure 11: Sub-sample analysis: responses of the GVA aggregate growth rate in cold and hot NUTS2 regions over the $2000 - 2019$ period.
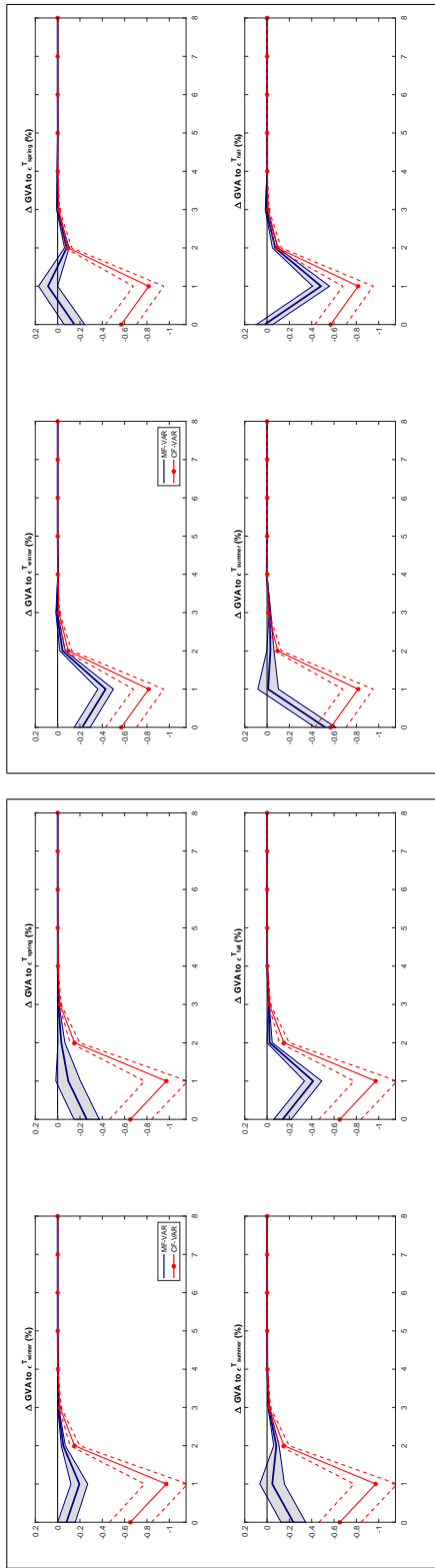
(a) Cold NUTS2 regions

(b) Hot NUTS2 regions

Notes. Impulse responses of the real GVA growth rate (ΔGVA) in percent, computed over an 8-year forecast horizon, for cold NUTS2 regions (panel a) and for hot NUTS2 regions (panel b), using the $2000 - 2019$ period as estimation sample. A region is labelled as a cold region if its average temperature is below the median, otherwise, the region falls into the hot region sub-group. The charts show the impulse response profile of ΔGVA to temperature shocks occurring in winter (ε_{winter}^T), spring (ε_{spring}^T), summer (ε_{summer}^T), and fall (ε_{fall}^T). Each chart displays the median response (blue line) and the corresponding 68% error bands (grey shadow area) computed by estimating the Panel MF-VAR described in equation (1). The size of the temperature shocks in each season is normalized to a 1°C increase in the temperature levels. The median response (red line with asterisk) obtained from the estimation of a Panel CF-VAR (fitted to annual temperature and real GVA growth rate) and the corresponding 68% error bands (red dashed lines) are also reported. For comparison, the size of the shock in the Panel CF-VAR is also normalized to a 1°C increase in the level of temperature.

24

MF-VAR show a more heterogenous intra-year response of ΔGVA. In particular, we find that, on impact, hotter regions are more affected by a temperature rise during summer (-0.52%) than colder regions (-0.24%). Also in winter, an increase in temperature levels is associated with a reduction in ΔGVA that is larger in hotter regions than in the colder ones, both on impact (-0.22% and -0.08%, respectively) and at horizon one (-0.43% and -0.20%, respectively). In contrast, in spring, on impact, the negative response of ΔGVA is slightly larger, in absolute values, in cold regions (-0.26%) than in hot regions (-0.15%), while both the responses become not statistically significant beyond time zero. Finally, in fall the negative response of ΔGVA is relatively large in cold regions (-0.14%), on impact, while it becomes similar in the two sub-groups at horizon one (-0.48% in hot regions and -0.41% in cold regions).

Furthermore, we repeat the empirical analysis by grouping the NUTS2 regions into two sub-groups based on the level of income. In line with Kahn et al. (2021), the regional income is proxied by the GVA at purchasing power parity (PPP) per capita. According to Kahn et al. (2021), a region is defined as a poor region if its average GVA PPP per capita (computed over the $2000 - 2019$ period) is below the median, while it is labelled as a rich region if its average (over $2000 - 2019$) GVA PPP per capita is above the median.[21] Poor and rich regions are shown in Figure 12. Figure 13 shows the responses of aggregate ΔGVA to an increase in temperature levels equal to $1°$C for poor (Figure 13, panel a) and rich (Figure 13, panel b) NUTS2 regions. The results obtained from the estimation of the Panel CF-VAR do not reveal evidence of a significant difference between poor and rich regions. In both sub-groups, we find a reduction of ΔGVA equal to around -0.5%, on impact, and to -0.9%, at horizon one, before reaching zero at further horizons. However, a closer inspection of the results obtained from the estimation of the Panel MF-VAR shows a larger reduction of economic activity in poor regions than in the rich ones, in almost all seasons. For example, in spring, while the response of ΔGVA is not statistically different from zero over the whole forecast horizon in rich regions, poor regions report a negative and statistically significant reduction of economic growth at horizon zero (-0.26%). Moreover, in winter and fall, both the two sub-groups show similar responses on impact, i.e. around -0.15% in winter and not statistically different from 0 in fall. However, at horizon one, the economic activity decreases more in poor regions than in rich ones: -0.41% and -0.28%, respectively (in winter), and -0.50% and -0.30%, respectively (in fall). The exception is the response of ΔGVA observed during summer. In particular, on impact, we find that the

---

[21]The median of the average $(2000 - 2019)$ GVA PPP per capita is equal to 20671.6 euro.

negative response of economic growth is larger in poor regions (-0.37%) than in the rich ones (-0.31%). However, whilst for poor regions, we observe a rebound effect at horizon one (0.17%), the response of economic growth remains negative also beyond time zero for rich regions.

Finally, the empirical exercise is conducted for two different sub-groups of NUTS2 regions that are constructed on the basis of their degree of competitiveness. As a proxy of regional competitiveness, we use the European Regional Competitiveness Index (RCI) produced by the European Commission which provides a synthetic measure of territorial competitiveness at a NUTS2 level. In particular, we use the 2010 version of the index for 216 EU NUTS2 regions.[22] The RCI 2010 is constructed by aggregating 11 pillars into three groups, that is basic, efficiency, and innovation.[23] This composite indicator reflects the region's level of development by highlighting basic issues in less developed regions and innovative capacity in more developed regions, with a focus on issues related both to firms and residents. The index takes values between 0 (lowest competitiveness degree) and 100 (highest competitiveness degree). The two sub-groups (highly and low competitive) are constructed as follows: if the assigned value of the RCI 2010 index for a region is below the median of the RCI 2010 distribution, then this region is labelled as highly competitive, while if the RCI 2010 index is below the median, the region is labelled as low competitive.[24] The two sub-groups are displayed in Figure 14. Figure 15 shows the responses of ΔGVA to temperature shocks (normalized to a 1°C increase in

---

[22]The RCI 2010 is available for 234 NUTS2 regions of 26 EU countries (plus 37 UK NUTS2 regions): Austria, Belgium, Bulgaria, Cyprus, Czech Republic, Germany, Denmark, Estonia, Spain, Finland, France, Greece, Hungary, Ireland, Italy, Lithuania, Luxembourg, Latvia, Malta, Netherlands, Poland, Portugal, Romania, Sweden, Slovenia, Slovakia. To compare the results obtained from the competitiveness analysis with those described in the rest of the paper, we first match the European Commission database with the dataset discussed in Section 3.1 (i.e., 225 NUTS2 regions). For a number of regions, the NUTS code reported in the RCI 2010 database is different from that displayed in the ARDECO dataset. This is due to changes in the NUTS codes that occurred in the various NUTS version since 2010 (at the time of writing this paper, the latest version is 2021). We replace the NUTS2 code of the RCI 2010 dataset with those reported in ARDECO when the match is possible by comparing the exact full name of the NUTS (i.e. recoding/relabelling). In contrast, we exclude from the final dataset (i.e., 225 NUTS2) the regions whose NUTS code does not match the one displayed in the ARDECO dataset, due to e.g., boundary change occurring among the administrative units. In particular, the following regions are removed from the sample (in bracket we report the ARDECO NUTS2 code): *Helsinki-Uusimaa* (FI1B), *Pohjois- ja Itä-Suomi* (FI1D), *Northern and Western* (IE04), *Southern* (IE05), *Eastern and Midland* (IE06), *Warszawski stoleczny* (PL91), *Mazowiecki regionalny* (PL92).

[23]The 11 pillars that are taken into account to construct the RCI 2010 are: institutions, macroeconomic stability, infrastructure, health, primary and secondary education, higher education, labor market efficiency, market size, tech readiness households, business sophistication, and innovation.

[24]The median RCI 2010 is equal to 56.2.

Figure 12: Poor and rich NUTS2 regions. Annual GVA PPP per capita over the $2000 - 2019$ time span.
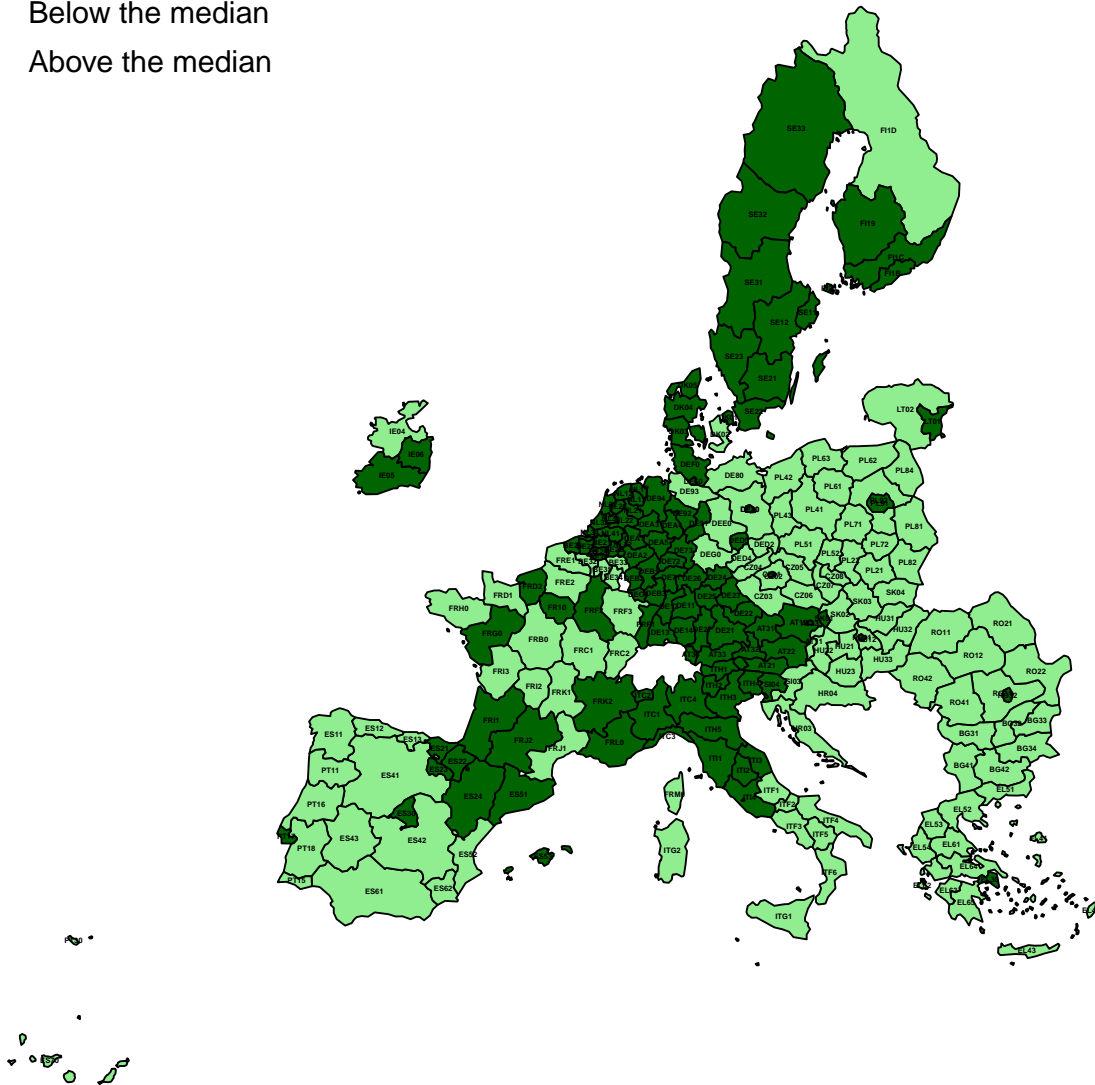
Notes. Annual GVA in purchasing power parity (PPP) per capita of the 225 EU NUTS2 regions averaged over the period $2000 - 2019$. A region is labelled as a poor region if its average GVA PPP per capita is below the median, otherwise, the region falls into the rich region sub-group. The median GVA PPP per capita is equal to 20671.6 euro. The Eurostat NUTS 2021 code for each region is also reported.

Figure 13: Sub-sample analysis: responses of the GVA aggregate growth rate in poor and rich NUTS2 regions over the $2000 - 2019$ period.
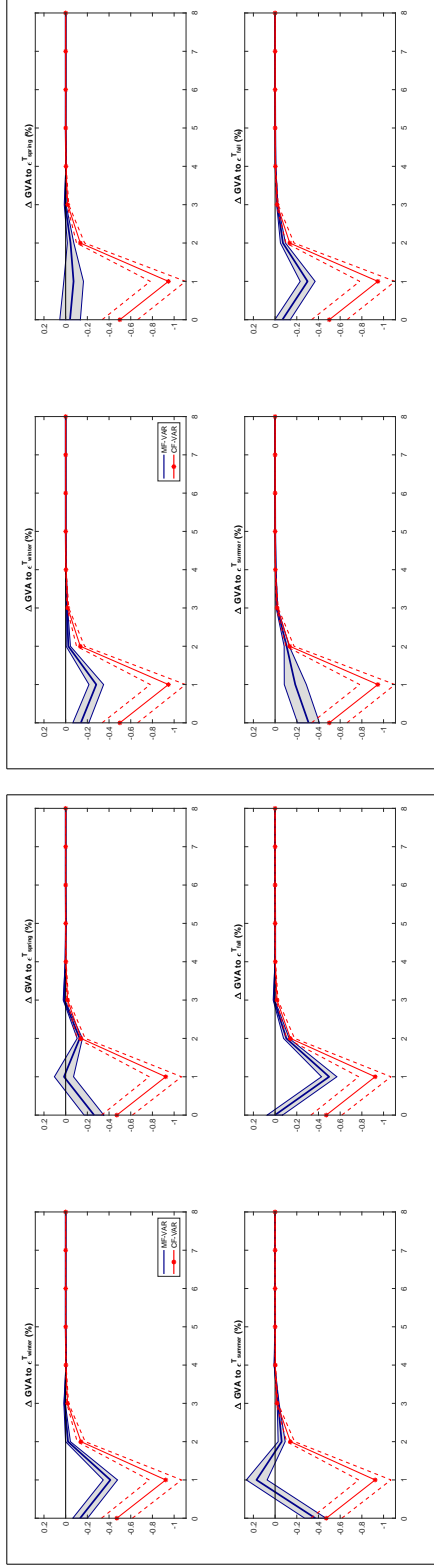
(a) Poor NUTS2 regions
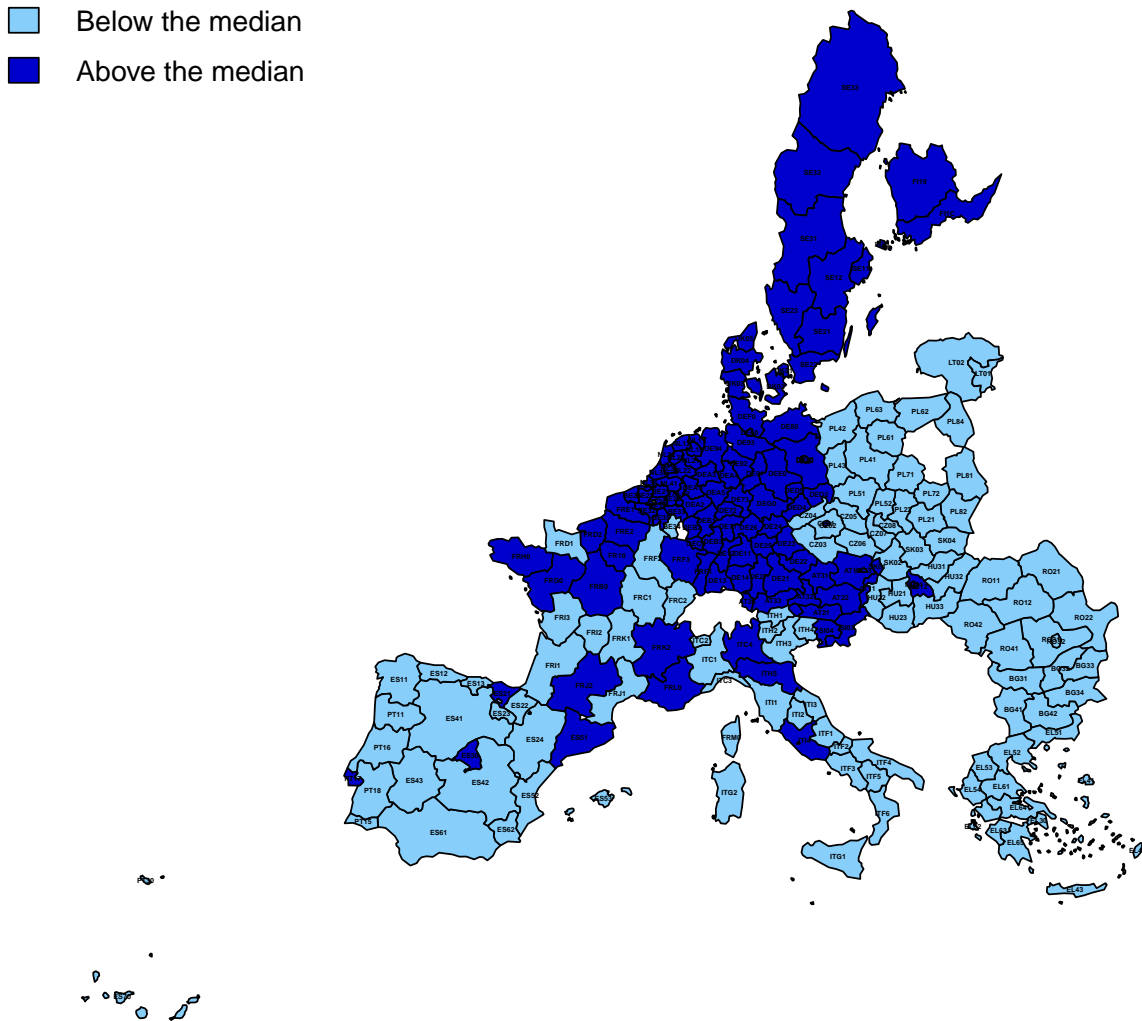

(b) Rich NUTS2 regions

Notes. Impulse responses of the real GVA growth rate (ΔGVA) in percent, computed over an 8-year forecast horizon, for poor NUTS2 regions (panel a) and for rich NUTS2 regions (panel b), using the $2000 - 2019$ period as estimation sample. A region is labelled as a poor region if its average GVA purchasing power parity (PPP) per capita is below the median, otherwise, the region falls into the rich region sub-group. The charts show the impulse response profile of ΔGVA to temperature shocks occurring in winter (ε^T_{winter}), spring (ε^T_{spring}), summer (ε^T_{summer}), and fall (ε^T_{fall}). Each chart displays the median response (blue line) and the corresponding 68% error bands (grey shadow area) computed by estimating the Panel MF-VAR described in equation (1). The size of the temperature shocks in each season is normalized to a 1°C increase in the temperature levels. The median response (red line with asterisk) obtained from the estimation of a Panel CF-VAR (fitted to annual temperature and real GVA growth rate) and the corresponding 68% error bands (red dashed lines) are also reported. For comparison, the size of the shock in the Panel CF-VAR is also normalized to a 1°C increase in the level of temperature.

temperature levels) in both low competitive (Figure 15, panel a) and highly competitive NUTS2 regions (Figure 15, panel b). As shown by Figure 15, the response of ΔGVA to annual temperature shocks (i.e., the response obtained from the Panel CF-VAR) is larger in low competitive regions than in the highly competitive ones, both on impact and at further forecast horizons. In particular, we find that on impact, the response of ΔGVA is equal to -0.33% in low competitive regions and to -0.18% in highly competitive regions. At horizon one (i.e., the negative peak in the response of ΔGVA), we observe a reduction in the proxy of economic activity of 0.84%, while economic growth decreases by 0.72% in highly competitive regions. A closer inspection of the seasonal results reveals that the negative response of ΔGVA in low competitive regions is larger in absolute values than those reported by highly competitive regions. This result is particularly evident in winter and in fall. In winter, the response of ΔGVA in low competitive regions is equal to -0.13% (on impact) and to -0.40% (at horizon one), while the corresponding results in highly competitive regions are 0.09% and -0.19%, respectively. In fall, we find that the cumulative response of ΔGVA over a two-year horizon (i.e., on impact and at horizon one) is equal to -0.47% in low competitive regions, while ΔGVA decreases by 0.28% in highly competitive regions, over the same forecast horizon. In spring and summer, the negative response of economic growth is larger in low competitive regions (-0.20% and -0.24%, respectively) than that reported by highly competitive regions (-0.06% and -0.21%, respectively). In contrast, at horizon one, we observe a rebound in the response of ΔGVA in low competitive regions, particularly pronounced in summer (0.32%), while the response in highly competitive regions remains negative also at horizon one (-0.11% in spring and -0.21% in summer).

4 Robustness check

Real GVA per capita. We repeat the empirical analysis by using the log changes of GVA per capita (ΔGVA p.c.) as a proxy of real economic activity. Figures 16-17 show the response of ΔGVA p.c. to a 1°C rise in the temperature levels across the 225 NUTS2 regions. Figure 16 shows the response of the proxy of economic activity over the full sample (i.e., $1981-2019$), while the responses of ΔGVA p.c. for the sub-sample period $2000-2019$ are reported in Figure 17. As can be seen from the two figures, the responses of ΔGVA p.c. are qualitatively and quantitatively similar to those obtained by estimating the models using ΔGVA, both over the full sample period (see Figure 2) and the sub-sample $2000-2019$ (see Figure 3).

Figure 14: Highly and low competitive NUTS2 regions. European Regional Competitiveness Index in 2010.

Notes. Regional Competitiveness Index (constructed by the European Commission) for 216 EU NUTS2 regions in 2010. A region is labelled as a low competitive region if its RCI 2010 is below the median, otherwise, the region is labelled as a highly competitive region. The median RCI 2010 is equal to 56.2. The Eurostat NUTS 2021 code for each region is also reported.

Figure 15: Sub-sample analysis: responses of the GVA aggregate growth rate in low and highly competitive NUTS2 regions over the $2000 - 2019$ period.
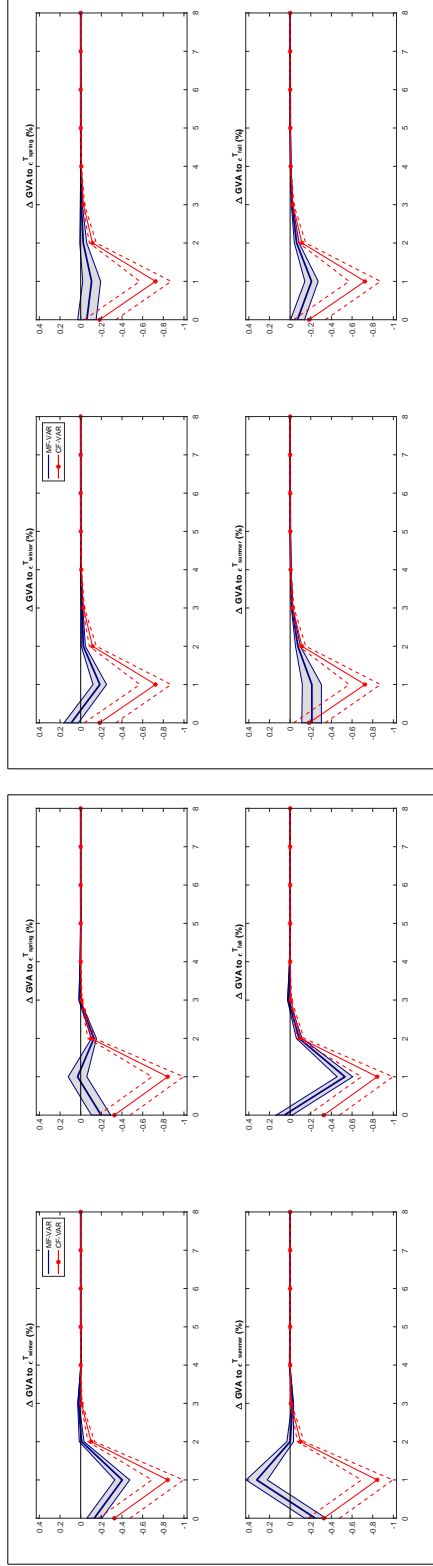
(a) Low competitive NUTS2 regions

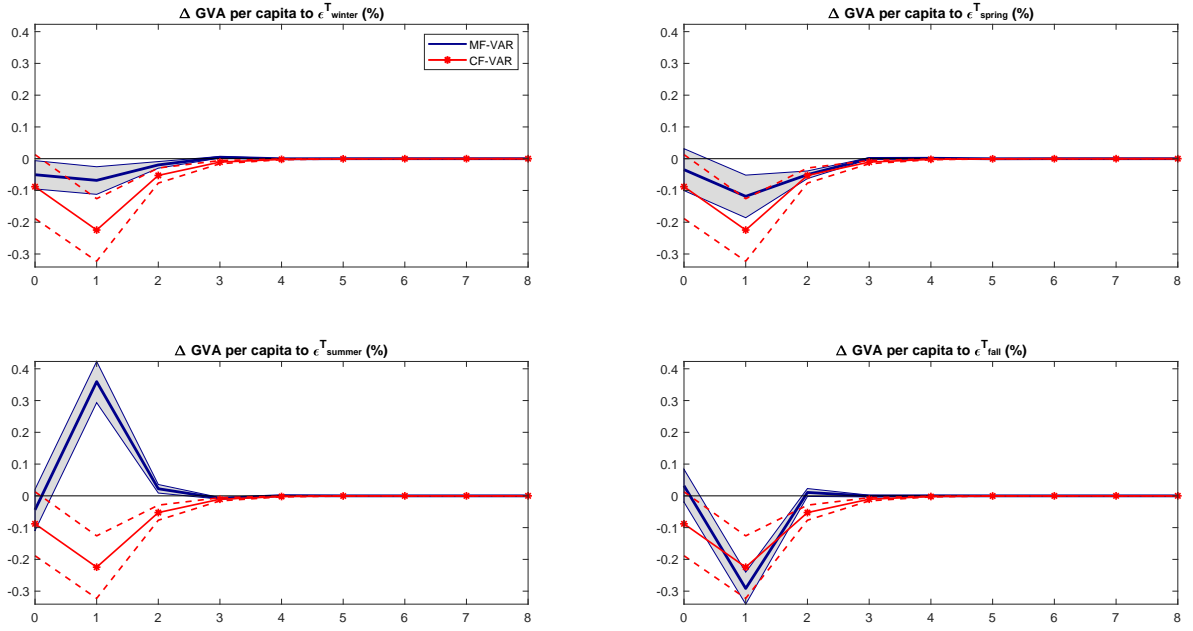**(b)** Highly competitive NUTS2 regions

Notes. Impulse responses of the real GVA growth rate (ΔGVA) in percent, computed over an 8-year forecast horizon, for low competitive NUTS2 regions (panel a) and for highly competitive NUTS2 regions (panel b), using the $2000 - 2019$ period as estimation sample. A region is labelled as a low competitive region if its RCI 2010 is below the median, otherwise, the region is labelled as a highly competitive region. The charts show the impulse response profile of ΔGVA to temperature shocks occurring in winter (ε^T_{winter}), spring (ε^T_{spring}), summer (ε^T_{summer}), and fall (ε^T_{fall}). Each chart displays the median response (blue line) and the corresponding 68% error bands (grey shadow area) computed by estimating the Panel MF-VAR described in equation (1). The size of the temperature shocks in each season is normalized to a 1°C increase in the temperature levels. The median response (red line with asterisk) obtained from the estimation of a Panel CF-VAR (fitted to annual temperature and real GVA growth rate) and the corresponding 68% error bands (red dashed lines) are also reported. For comparison, the size of the shock in the Panel CF-VAR is also normalized to a 1°C increase in the level of temperature.

31

Over the full sample period, the results from the estimation of the Panel CF-VAR reveal a reduction of ΔGVA p.c. of 0.08% (although the response is not statistically significant), on impact. The response ΔGVA p.c. at its peak (i.e., at horizon one) is negative and statistically significant, reporting a value of -0.22% (as in the response of ΔGVA). On impact, similar to the results for ΔGVA, the response of ΔGVA p.c. is negative in winter (-0.05%) and in summer (-0.04%). However, we find that only the response in winter is statistically significant. Moreover, as in the case of ΔGVA, we observe that the response of ΔGVA p.c. is not statistically significant in spring and in fall. At horizons greater than zero, the impulse response profile of the ΔGVA p.c. is similar to that observed for ΔGVA. At horizon one (i.e., its peak), the response is negative in winter (-0.07%), in spring (-0.12%), and in fall (-0.29%), while in summer we find the same rebound effect (0.4%) observed for ΔGVA.

We now turn the focus to the results obtained from the estimation of the Panel MF- and CF-VARs using the last 20 years of the sample (that is $2000-2019$). As can be seen in Figure 17, the results from the Panel CF-VAR are similar to those obtained for ΔGVA. In particular, we find a reduction of 0.66%, on impact (-0.61% is the response of ΔGVA), and of 0.99%, at horizon one (-0.97% is the response of ΔGVA). Likewise, the response ΔGVA p.c. observed during the four seasons are similar to those described in Section 3.2. In particular, we find that, on impact, the largest reduction of ΔGVA p.c. is observed in summer (-0.41%). The responses in the remaining seasons are smaller than the ones observed in summer, but qualitatively and quantitatively similar to the estimates obtained for ΔGVA: winter (-0.18%), spring (-0.17%), and fall (-0.10%). Moreover, similar to the responses obtained for ΔGVA, we find that winter (-0.38%) and fall (-0.42%) are the seasons that contribute the most to the reduction of ΔGVA p.c. at horizon one (i.e., the peak of the response of ΔGVA p.c.).
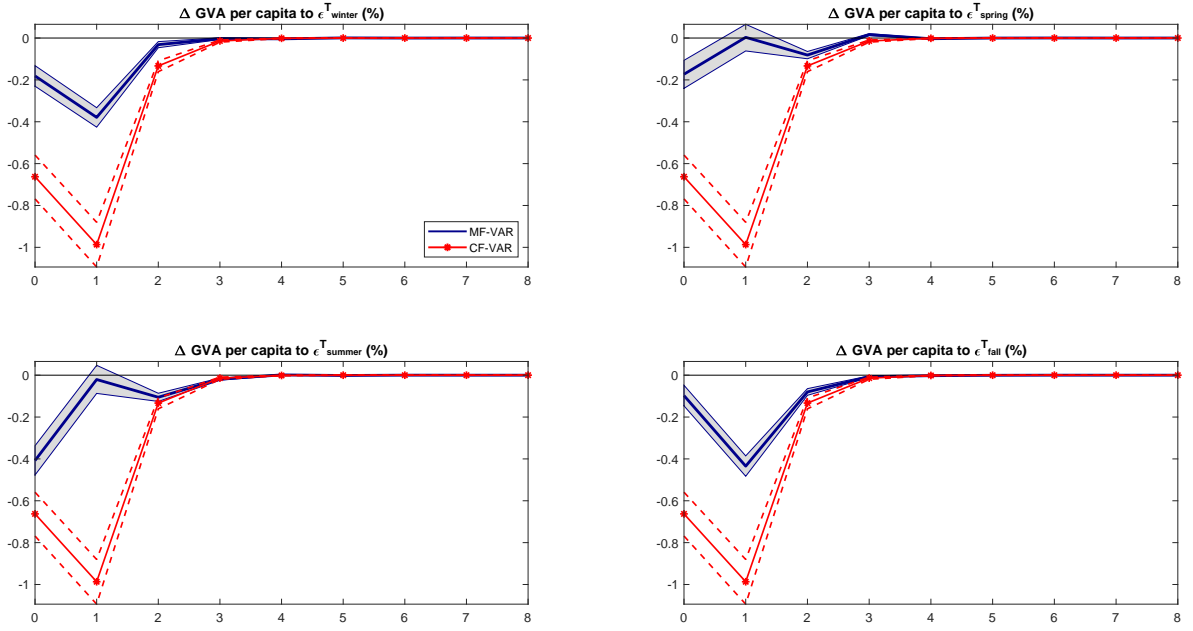
Rolling window estimation. In Section 3.2, we discuss the impulse response profile of economic activity to temperature shocks over the $2000-2019$ sub-sample period. We also explore the results obtained over previous rolling sub-samples and we report the results in Figure 18. To avoid clutter, we plot the median estimate, together with the 68% error bands, only for horizon 0 (i.e., contemporaneous impact) and for horizon 1. As can be seen in Figure 18, we find that the negative effect (at horizons 0 and 1) of annual temperatures on output increases over time, reaching its peak over the last 20 years, i.e., 2000-2019 (panel a). Moreover, the mixed-frequency analysis reveals that temperature shocks in summer and winter contribute the most to this worsening of macroeconomic conditions (panel b).

**Figure 16:** Responses of the regional real GVA per capita growth over the $1981 - 2019$ period.

Notes. Impulse responses of the real GVA per capita growth rate (ΔGVA p.c.) in percent, computed over an 8-year forecast horizon, using the $1981 - 2019$ period as an estimation sample. The charts show the impulse response profile of ΔGVA p.c. to temperature shocks occurring in winter (ε_{winter}^{T}), spring (ε_{spring}^{T}), summer (ε_{summer}^{T}), and fall (ε_{fall}^{T}). Each chart displays the median response (blue line) and the corresponding 68% error bands (grey shadow area) computed by estimating the Panel MF-VAR described in equation (1). The size of the temperature shocks in each season is normalized to a 1°C increase in the temperature levels. The median response (red line with asterisk) obtained from the estimation of a Panel CF-VAR (fitted to annual temperature and ΔGVA p.c.) and the corresponding 68% error bands (red dashed lines) are also reported. For comparison, the size of the shock in the Panel CF-VAR is also normalized to a 1°C increase in the level of temperature.

Figure 17: Sub-sample analysis: responses of the regional real GVA per capita growth over the $2000 - 2019$ period.


Notes. Impulse responses of the real GVA per capita growth rate (ΔGVA p.c.) in percent, computed over an 8-year forecast horizon, using the $2000 - 2019$ period as an estimation sample. The charts show the impulse response profile of ΔGVA p.c. to temperature shocks occurring in winter (ε^T_{winter}), spring (ε^T_{spring}), summer (ε^T_{summer}), and fall (ε^T_{fall}). Each chart displays the median response (blue line) and the corresponding 68% error bands (grey shadow area) computed by estimating the Panel MF-VAR described in equation (1). The size of the temperature shocks in each season is normalized to a 1°C increase in the temperature levels. The median response (red line with asterisk) obtained from the estimation of a Panel CF-VAR (fitted to annual temperature and ΔGVA p.c.) and the corresponding 68% error bands (red dashed lines) are also reported. For comparison, the size of the shock in the Panel CF-VAR is also normalized to a 1°C increase in the level of temperature.

Figure 18: Impulse responses through rolling window estimation.
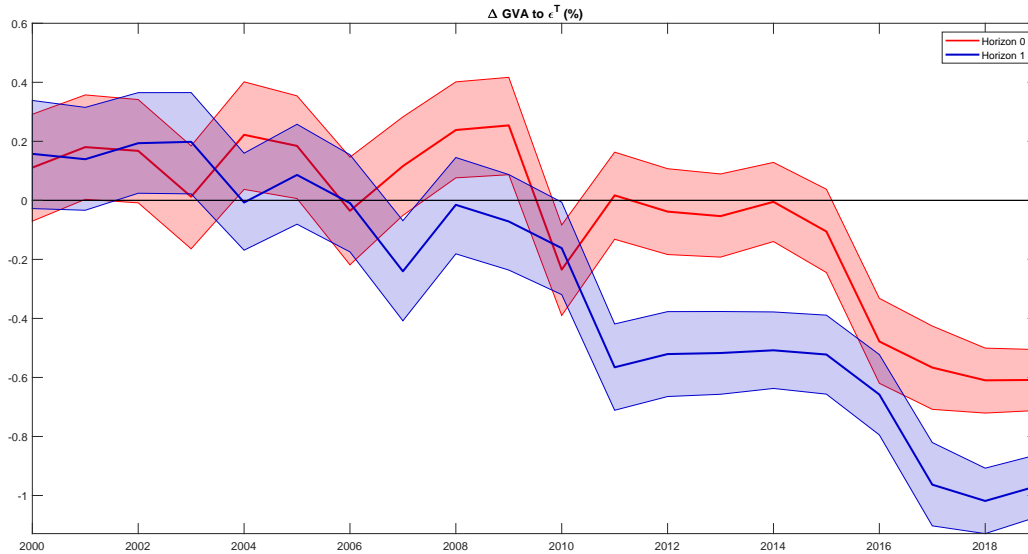
(a) Common-frequency
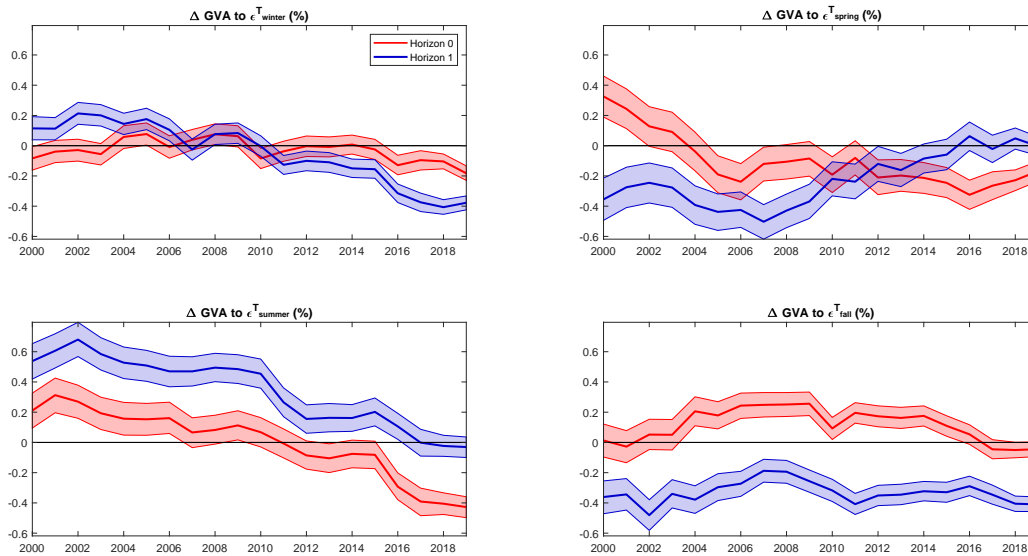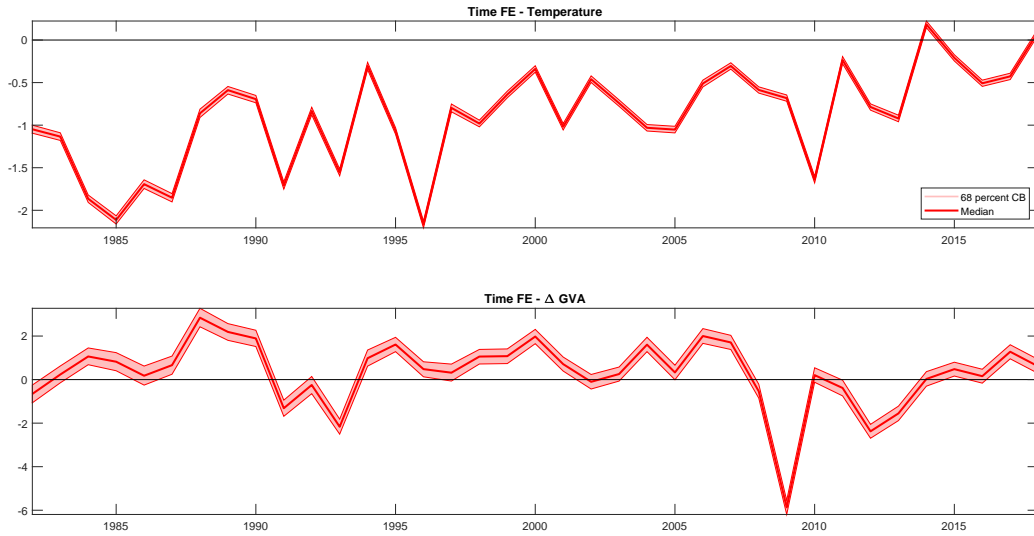
(b) Mixed-frequency

Notes. Impulse responses computed by estimating a Panel CF-VAR (panel a) and a Panel MF-VAR (panel b) over a 20-year rolling window estimation sample. Median response for horizon 0 (red line) and for horizon 1 (blue line) with the corresponding 68% error bands are reported. First estimation sample: $1981-2000$.

35

Global Financial Crisis. To check whether the results discussed in Section 3.2 are driven by large common shocks that occurred over the observed sample periods, such as the global financial crisis (GFC), we plot the parameters associated with the year-fixed effects obtained from the estimation of the mixed- and common-frequency models using data both for the $1981 - 2019$ (Figure 19) and the $2000 - 2019$ (Figure 20) sample periods. As can be seen in Figures 19-20, the inclusion of the year-fixed effects in the model specification allows us to filter out the role played by the GFC in driving the reduction of economic activity in response to temperature shocks.

5   Conclusions

In this study, we examine the annual and seasonal temperature effects on growth using a Panel Mixed-Frequency VAR fitted to 225 EU regions. The empirical evidence shows an increase in the detrimental effect of temperature on growth, especially during the most recent sub-sample (spanning $2000 - 2019$), spreading throughout different sectors and mostly for hot, poor, and less competitive regions. Finally, our findings show that EU climate policy action should not consider and target mainly agriculture, forestry, and fishing sectors, but also construction, industry, and services.

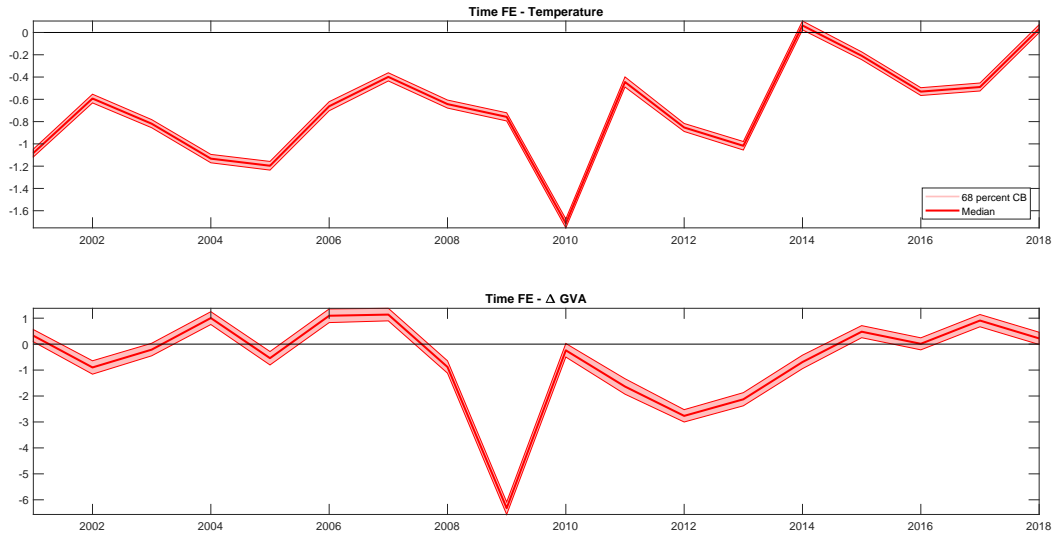**Figure 19:** Time-fixed effects over $1981 - 2019$.
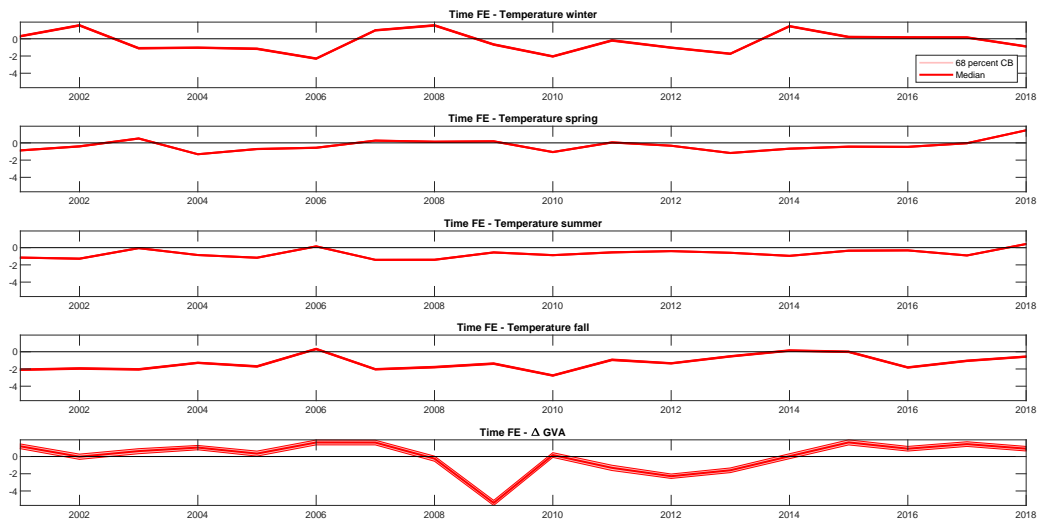

(a) Common-frequency
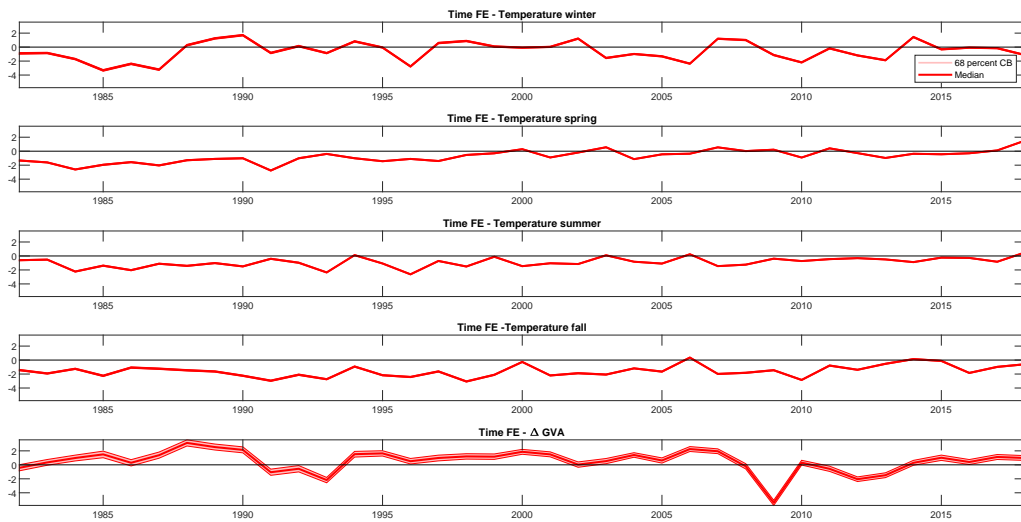
(b) Mixed-frequency

Notes. Time-fixed effects obtained from the estimation of the Panel CF-VAR (panel a) and of the panel MF-VAR (panel b) using data for the $1981 - 2019$ time span. Median response (red line) with 68% (red shading) error bands are reported.

Figure 20: Time-fixed effects over $2000 - 2019$.

(a) Common-frequency

(b) Mixed-frequency

Notes. Time-fixed effects obtained from the estimation of the Panel CF-VAR (panel a) and of the panel MF-VAR (panel b) using data for the $2000 - 2019$ time span. Median response (red line) with 68% (red shading) error bands are reported.

References

Acevedo, S., Mrkaic, M., Novta, N., Pugacheva, E., & Topalova, P. (2020). The Effects of Weather Shocks on Economic Activity: What are the Channels of Impact? *Journal of Macroeconomics*, *65*, 103207.

Alessandri, P., & Mumtaz, H. (2021). The Macroeconomic Cost of Climate Volatility. *Queen Mary University of London, School of Economics and Finance Working Paper No. 928*.

Bańbura, M., Giannone, D., & Reichlin, L. (2010). Large Bayesian vector auto regressions. *Journal of Applied Econometrics*, *25*(1), 71–92.

Bansal, R., Ochoa, M., & Kiku, D. (2016). Climate Change and Growth Risks. *NBER Working Paper No. 23009, National Bureau of Economic Research*.

Beetsma, R., Furtuna, O., Giuliodori, M., & Mumtaz, H. (2021). Revenue-versus spending-based fiscal consolidation announcements: Multipliers and follow-up. *Journal of International Economics*, *131*, 103455.

Burke, M., Davis, W. M., & Diffenbaugh, N. S. (2018). Large potential reduction in economic damages under UN mitigation targets. *Nature*, *557*, 549–553.

Burke, M., Hsiang, S. M., & Miguel, E. (2015). Global non-linear effect of temperature on economic production. *Nature*, *527*, 235–239.

Burke, M., & Tanutama, V. (2019). Climatic Constraints on Aggregate Economic Output. *NBER Working Paper No. 25779, National Bureau of Economic Research*.

Canova, F., & Ciccarelli, M. (2013). Panel Vector Autoregressive Models: A Survey. In *VAR Models in Macroeconomics - New Developments and Applications: Essays in Honor of Christopher A. Sims (Advances in Econometrics, Vol. 32)* (pp. 205–246).

Ciccarelli, M., & Marotta, F. (2021). Demand or supply? An empirical exploration of the effects of climate change on the macroeconomy. *ECB Working Paper No. 2608*.

Colacito, R., Hoffmann, B., & Phan, T. (2019). Temperature and Growth: A Panel Analysis of the United States. *Journal of Money, Credit and Banking*, *51*(2-3), 313–368.

Dell, M., Jones, B. F., & Olken, B. A. (2012). Temperature Shocks and Economic Growth: Evidence from the Last Half Century. *American Economic Journal: Macroeconomics*, *4*(3), 66–95.

Deryugina, T., & Hsiang, S. M. (2014). Does the Environment Still Matter? Daily Temperature and Income in the United States. *NBER Working Paper No. 20750, National Bureau of Economic Research*.

Donadelli, M., Grüning, P., Jüppner, M., & Kizys, R. (2021). Global temperature, R&D expenditure, and growth. *Energy Economics*, *104*, 105608.

Ghysels, E. (2016). Macroeconomics and the reality of mixed frequency data. *Journal of Econometrics*, *193*(2), 294–314.

Greßer, C., Meierrieks, D., & Stadelmann, D. (2021). The link between regional temperature and regional incomes: econometric evidence with sub-national data. *Economic Policy*, *36*(107), 523–550.

Kahn, M. E., Mohaddes, K., Ng, R. N., Pesaran, M. H., Raissi, M., & Yang, J.-C. (2021). Long-term macroeconomic effects of climate change: A cross-country analysis. *Energy Economics*, *104*, 105624.

Kalkuhl, M., & Wenz, L. (2020). The impact of climate conditions on economic production. Evidence from a global panel of regions. *Journal of Environmental Economics and Management*, *103*, 102360.

Kotz, M., Wenz, L., Stechemesser, A., Kalkuhl, M., & Levermann, A. (2021). Day-to-day temperature variability reduces economic growth. *Nature Climate Change*, *11*, 319–325.

Li, N., Bai, K., Zhang, Z., Feng, J., Chen, X., & Liu, L. (2019). The nonlinear relationship between temperature changes and economic development for individual provinces in China. *Theoretical and Applied Climatology*, *137*, 2477–2486.

Marcellino, M. (1999). Some Consequences of Temporal Aggregation in Empirical Analysis. *Journal of Business & Economic Statistics*, *17*(1), 129–136.

Mohaddes, K., Ng, R. N. C., Pesaran, M. H., Raissi, M., & Yang, J.-C. (2022). Climate Change and Economic Activity: Evidence from U.S. States. *Oxford Open Economics*, *Forthcoming*.

Olper, A., Maugeri, M., Manara, V., & Raimondi, V. (2021). Weather, climate and economic outcomes: Evidence from Italy. *Ecological Economics*, *189*, 107156.

Zhao, X., Gerety, M., & Kuminoff, N. V. (2018). Revisiting the temperature-economic growth relationship using global subnational data. *Journal of Environmental Management*, *223*, 537–544.

Appendices

Appendix A. Bayesian estimation

The Natural conjugate prior is imposed on the VAR coefficients by augmenting the system in equation (1) with a set of artificial dummy observations, which are specified as follows:

$$
\underset{(Kp+m+K)\times K}{Y_d} = \begin{pmatrix} diag(\frac{\delta_1\sigma_1,\ldots,\delta_K\sigma_K}{\lambda}) \\ 0_{K(p-1)\times K} \\ \ldots \\ diag(\sigma_1,\ldots,\sigma_K) \\ \ldots \\ 0_{m\times K} \end{pmatrix}, \quad \underset{(Kp+m+K)\times(Kp+m)}{X_d} = \begin{pmatrix} J_p \otimes diag(\frac{\sigma_1,\ldots,\sigma_K}{\lambda}) & 0_{Kp\times m} \\ \ldots & \ldots \\ 0_{K\times Kp} & 0_{K\times m} \\ \ldots & \ldots \\ 0_{m\times Kp} & diag(\eta) \end{pmatrix}
$$

$$\tag{A.1}$$

where $J_p = diag(1,\ldots,p)$, δ_i, for $i = 1,\ldots,K$, are the prior mean of the VAR parameters associated with the lag of order one, σ_i, for $i = 1,\ldots,K$, are scaling factors (i.e., accounting for the different scales of the endogenous variables), λ controls for the overall tightness around the prior of the VAR coefficients and η controls the prior for the m exogenous variables included in equation (1) (that is the region- and time-fixed effects). We set the prior means (δ_i) and the scaling factors (σ_i) equal to, respectively, the coefficient and the residual standard deviation obtained from the OLS estimation of an AR(1) model fitted to each endogenous variable. Moreover, λ and η are set equal to 1 and 1/10000, respectively, to reflect a loose prior on both the slope coefficients and the exogenous variables.

After pooling the observations (i.e., the Panel MF-VAR is treated as a MF-VAR), the model in equation (1) can be written in matrix notation as follows:

$$Y = XB + U \tag{A.2}$$

where $Y = (Y_1,\ldots,Y_T)'$ is a $NT \times K$ matrix containing the K endogenous variables, with N being the number of NUTS2 regions. Furthermore, $X = (X_1,\ldots,X_T)'$ is the $NT \times (Kp + m)$ matrix of lagged endogenous variables and of region- and time-fixed effects, that is $X_t = [Y'_{t-1},\ldots,Y'_{t-\ell}, \mathbf{1_i}', d'_t]$, $B = (A_1,\ldots,A_\ell,\alpha_i,\beta)'$ and $U = (u_1,\ldots,u_T)'$, with $U \sim \mathcal{N}(0,\Sigma)$. As described in Bańbura et al. (2010), the Normal-inverse Wishart distribution can be implemented by augmenting the model in equation (A.2) with the

dummy observations Y_d and X_d reported in equation (A.1):

$$Y^* = X^* B + U^* \tag{A.3}$$

where $Y^* = (Y', Y_d')'$, $X^* = (X', X_d')'$, $U^* = (U', U_d')'$. The conditional posterior distribution for the VAR coefficients (B) and the residual covariance matrix (Σ) can be written as follows:

$$vec(B)|\Sigma, Y \sim \mathcal{N}\Big(vec(B^*),\ \Sigma \otimes (X^{*'} X^*)^{-1}\Big) \tag{A.4}$$
$$\Sigma|Y \sim \mathcal{IW}\Big(S^*,\ v^*\Big)$$

where $B^* = (X^{*'} X^*)^{-1} X^{*'} Y^*$ is obtained from the OLS estimation of the augmented regression in equation (A.3), $S^* = (Y^* - X^* B^*)'(Y^* - X^* B^*)$ and $v^* = NT + T_d - K$ are the scale matrix and the degrees of freedom of the inverse Wishart distribution. The conditional posterior distribution is simulated using a standard Gibbs sampling algorithm, where the number of draws is set equal to 25000, with a burn-in phase of 15000 draws.

## Appendix B. Ex-post convergence

To assess the convergence of the Gibbs sampling algorithm, we compute the inefficiency factor for the Panel MF-VAR parameters (including slope coefficients and region-year fixed effects) and for the elements of the residual covariance matrix. In this appendix, we report the inefficiency factor computed for the Panel MF-VAR fitted to the four seasonal series of temperature levels and to the log changes of GVA, over the periods $1981 - 2019$ (Figure B.1) and $2000 - 2019$ (Figure B.2). To compute the inefficiency factor, we use a lag length of the sample autocorrelation equal to 20. As can be seen from Figures B.1-B.2, the inefficiency factor computed for the Panel MF-VAR parameters (upper panel) and for the elements of the residual covariance matrix (lower panel) is relatively low, suggesting convergence of the Gibbs sampling algorithm.

Figure B.1: Inefficiency factor from the estimation of the Panel MF-VAR using data over $1981 - 2019$.
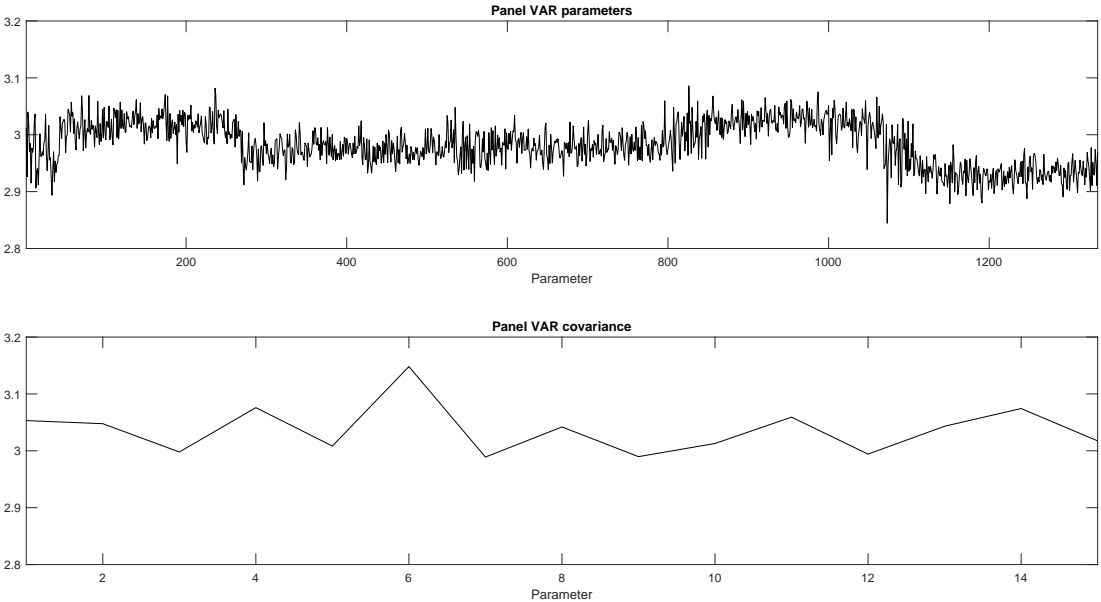
Notes. Inefficiency factor computed for the Panel MF-VAR parameters (upper panel) and the residual covariance matrix (lower panel) over the retained 10000 draws. The parameters (slope coefficients and region-year fixed effects) and the residual covariance matrix are obtained from the estimation of a Panel MF-VAR fitted to the four seasonal series of temperature levels and the log changes of GVA, over the $1981 - 2019$ time span. The inefficiency factor is computed using a lag length of the sample autocorrelation of order 20.

Figure B.2: Inefficiency factor from the estimation of the Panel MF-VAR using data over the sub-sample $2000 - 2019$.
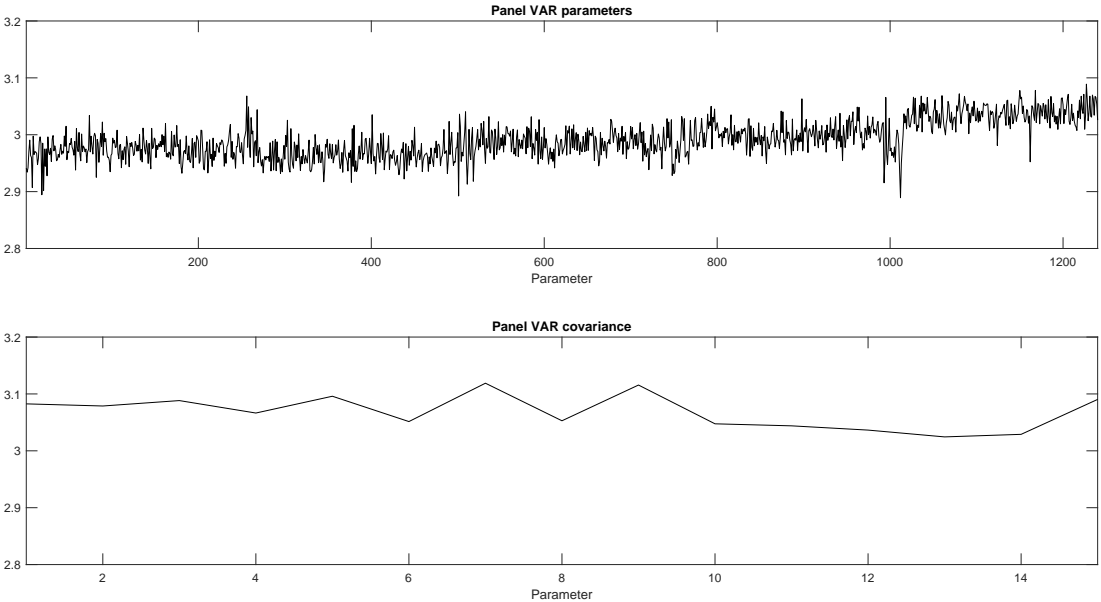
Notes. Inefficiency factor computed for the Panel MF-VAR parameters (upper panel) and the residual covariance matrix (lower panel) over the retained 10000 draws. The parameters (slope coefficients and region-year fixed effects) and the residual covariance matrix are obtained from the estimation of a Panel MF-VAR fitted to the four seasonal series of temperature levels and the log changes of GVA, over the $2000 - 2019$ time span. The inefficiency factor is computed using a lag length of the sample autocorrelation of order 20.

RECent Working Papers Series

The 10 most RECent releases are:

No. 154	NATURAL DISASTERS AND PREFERENCES FOR THE ENVIRONMENT: EVIDENCE FROM THE IMPRESSIONABLE YEARS (2022) C. Faco, R. Corbi
No. 153	DOES WAR MAKE STATES? MILITARY SPENDING AND THE ITALIAN STATE BUILDING, 1861-1945 (2022) A. Incerpi, B. Pistoresi, F. Salsano
No. 152	STRANGERS AND FOREIGNERS: TRUST AND ATTITUDES TOWARD CITIZENSHIP (2022) G. Bertocchi, A. Dimico, G. L. Tedeschi
No. 151	ADAMS AND EVES: THE GENDER GAP IN ECONOMICS MAJORS (2021) G. Bertocchi, L. Bonacini, M. Murat
No. 150	CHOOSE THE SCHOOL, CHOOSE THE PERFORMANCE. NEW EVIDENCE ON THE DETERMINANTS OF STUDENT PERFORMANCE IN EIGHT EUROPEAN COUNTRIES (2021) L. Bonacini, I. Brunetti, G. Gallo
No. 149	COVID-19, RACE, AND GENDER (2021) G. Bertocchi, A. Dimico
No. 148	MACROECONOMIC UNCERTAINTY AND VECTOR AUTOREGRESSIONS (2020) M. Forni, L. Gambetti, L. Sala
No. 147	COMMON COMPONENTS STRUCTURAL VARS (2020) M. Forni, L. Gambetti, M. Lippi, L. Sala
No. 146	ASYMMETRIC EFFECTS OF MONETARY POLICY EASING AND TIGHTENING (2020) D. Debortoli, M. Forni, L. Gambetti, L. Sala
No. 145	COVID-19, RACE, AND REDLINING (2020) G. Bertocchi, A. Dimico

The full list of available working papers, together with their electronic versions, can be found on the RECent website: http://www.recent.unimore.it/site/home/publications/working-papers.html